The *HST* Key Project on the Extragalactic Distance Scale XVII. The Cepheid Distance to the Coma II Group Galaxy NGC 4725[1]

Brad K. Gibson[2], Shaun M.G. Hughes[3], Peter B. Stetson[4], Laura Ferrarese[5], Holland Ford[6], Wendy L. Freedman[7], John A. Graham[8], Mingsheng Han[9], John G. Hoessel[9], John Huchra[10], Garth D. Illingworth[11], Robert C. Kennicutt, Jr.[12], Barry F. Madore[13], Jeremy R. Mould[2], Randy Phelps[7], Abhijit Saha[14], Shoko Sakai[13] and Nancy A. Silbermann[13]

Received ______________________; accepted ______________________

---

[1]Based on observations with the NASA/ESA *Hubble Space Telescope*, obtained at the Space Telescope Science Institute, which is operated by AURA, Inc., under NASA Contract No. NAS 5-26555.

[2]Mount Stromlo & Siding Spring Observatories, Australian National University, Weston Creek Post Office, Weston, ACT, Australia 2611

[3]Royal Greenwich Observatory, Madingley Road., Cambridge, UK CB3 0EZ
Current address: Institute of Astronomy, Madingley Road., Cambridge, UK CB3 0HA

[4]Dominion Astrophysical Observatory, Herzberg Institute of Astrophysics, National Research Council, 5071 West Saanich Rd., Victoria, BC, Canada V8X 4M6

[5]Palomar Observatory, California Institute of Technology, Pasadena, CA, USA 91125

[6]Dept. of Physics & Astronomy, Bloomberg 501, Johns Hopkins Univ., 3400 N. Charles St., Baltimore, MD, USA 21218

[7]The Observatories, Carnegie Institution of Washington, Pasadena, CA, USA 91101

[8]Dept. of Terrestrial Magnetism, Carnegie Institution of Washington, 5241 Broad Branch Rd. N.W., Washington, D.C., USA 20015

[9]Univ. of Wisconsin, Madison, WI, USA, 53706

[10]Harvard College, Center for Astrophysics, 60 Garden St., Cambridge, MA, USA 02138

[11]Lick Observatory, Univ. of California, Santa Cruz, CA, USA 95064

[12]Steward Observatory, Univ. of Arizona, Tucson, AZ, USA 85721

[13]Infrared Processing and Analysis Center, Jet Propulsion Laboratory, California Institute of Technology, Pasadena, CA, USA 91125

[14]Space Telescope Science Institute, 3700 San Martin Dr., Baltimore, MD, USA 21218

Submitted to ApJ, Part I

ABSTRACT

The distance to NGC 4725 has been derived from Cepheid variables, as part of the *Hubble Space Telescope Key Project on the Extragalactic Distance Scale.* Thirteen F555W (~V) and four F814W (~I) epochs of cosmic ray split Wide Field and Planetary Camera 2 observations were obtained. Twenty Cepheids were discovered, with periods ranging from ~ 14 to ~ 49 days. Adopting a Large Magellanic Cloud distance modulus and extinction of 18.50 ± 0.10 mag and E(V-I)=0.13 mag, respectively, a true reddening-corrected distance modulus (based on an analysis employing the ALLFRAME software package) of 30.50 ± 0.17 (random) $\pm$ 0.17 (systematic) mag was determined for NGC 4725, corresponding to a distance of 12.6 ± 1.0 (random) $\pm$ 1.0 (systematic) Mpc. Based upon 19 galaxies with Cepheid-derived distances, our interim infrared Tully-Fisher relationship calibration is given by $H^{abs}_{-0.5} = -21.48 - 10.13(\log \Delta V - 2.5)$. While consistent with previously published planetary nebula and globular cluster luminosity function distances, our Cepheid distance to NGC 4725 is inconsistent with that derived from surface brightness fluctuations, at the $\sim 3\sigma$ level.

Subject headings: galaxies: individual (NGC 4725) — galaxies: distances — stars: Cepheids

1. Introduction

The *Hubble Space Telescope (HST) Key Project on the Extragalactic Distance Scale* has as its primary goal the determination of the Hubble constant to an accuracy $\lesssim 10\%$ (Kennicutt, Freedman & Mould 1995). Cepheid distances to 18 spirals, within ~ 20 Mpc, are being obtained and will be used to calibrate a variety of secondary distance indicators, including the Tully-Fisher relation (TF), surface brightness fluctuations (SBF), planetary nebula luminosity function (PNLF), globular cluster luminosity function (GCLF), and Type Ia supernovae.

NGC 4725 is an Sb/SB(r)II barred spiral (Sandage 1996), with an uncorrected HI 21cm linewidth of $\sim$ 411 km/s (Wevers et al. 1984), and an isophotal inclination of $\sim 46°$ (de Vaucouleurs et al. 1991 - although, see Section 5.1.1). Based upon eight HII regions, Zaritsky, Kennicutt & Huchra (1994) determined a mean oxygen abundance of $12 + \log(\mathrm{O/H}) = 9.26 \pm 0.57$, at a galactocentric distance $r = 3$ kpc, with a corresponding abundance gradient of -0.022 ± 0.063 dex/kpc. Its position ($\alpha = 12^{h}50^{m}27^{s}, \delta = +25°30'06''$, J2000) and Galactocentric radial velocity $v = 1206$ km/s (de Vaucouleurs et al. 1991) place it within the Coma-Sculptor Cloud. NGCs 4725 and 4747 are relatively isolated dynamically from the remainder of the Cloud (e.g. Zaritsky et al. 1997), and comprise what has come to be known as the Coma II Group of galaxies (e.g. Table II of Tully 1988). NGC 4725 is one of the *HST Key Project* primary calibrators for the infrared Tully-Fisher (IRTF) relationship. Because of the (assumed) association of the Coma II Group with that of the Coma I Group[15] (and, to some degree, the Coma-Sculptor Cloud as a whole), NGC 4725 may indirectly provide calibration for the SBF, PNLF, and GCLF secondary candles. NGC 4725 was the host galaxy for supernova SN1940B, a typical example of the "regular" class of "plateau" Type II events (Patat et al. 1994), but data does not exist which would allow application of the expanding photosphere method secondary distance indicator.

In Section 2 we present our multi-epoch Wide Field and Planetary Camera 2 (WFPC2) *HST* observations and review the two independent approaches taken to the photometry and calibration of the instrumental magnitudes – the methodology employed follows that of previous papers in this series (e.g. Hill et al. 1998, and references therein). The identification of Cepheids and their intrinsic properties, again employing two independent algorithms, is discussed in Section 3. The derived distance to NGC 4725 is presented in Section 4, and the result contrasted with previous distance determinations for NGC 4725

[15]After Tully (1988), the Coma I Group is comprised of 25 members, including notables such as NGCs 4278, 4414 (although, see Section 5), 4494, and 4565.

and the Coma I/II groups of galaxies, in Section 5. A summary is provided in Section 6.

2. Observations and Photometry

HST WFPC2 observations of NGC 4725 were carried out over a two month period (12/04/95-14/06/95), with a single epoch revisit on 29/04/96. In total, thirteen epochs of F555W (∼V), four epochs of F814W (∼I), and two epochs of F439W (∼B) were covered. Each epoch consisted of a pair of cosmic-ray split exposures, each of duration 1000-1500 s. In addition, short exposure (i.e. , 230 s), single-epoch, observations were taken in each filter, to tie the observations to ground-based data. Because of the sparse phase coverage of the F439W observations, these were not included in the analysis which follows. The observing strategy, optimized to uncover Cepheids with periods $\sim 10-60$ days, follows that outlined in Kennicutt et al. (1995). The individual epochs, *HST* archive filenames, time at which a given epoch's observations began, and the exposure times and filters employed, are all listed in Table 1.

EDITOR: PLACE TABLE 1 HERE.

A $10' \times 10'$ ground-based image, obtained with the 2.5m Isaac Newton Telescope by one of the authors (SMGH), is shown in Figure 1; the WFPC2 footprint has been superimposed. WFPC2 incorporates four 800 × 800 CCDs; the Planetary Camera (PC) has a 36.8 × 36.8 arcsecond field of view, and is referred to as Chip 1, while the three Wide Field (WF) chips have 80 × 80 arcsecond fields of view each, and are referred to as Chips 2, 3, and 4, respectively, moving counter-clockwise from the PC in Figure 1.

EDITOR: PLACE FIGURE 1 HERE.

As in previous papers in this series, dual independent analyses were undertaken using ALLFRAME (Stetson 1994) and DoPHOT (Saha et al. 1996, and references therein). As detailed descriptions of the reduction process can be found in Ferrarese et al. (1996) and Hill et al. (1998), we only provide a brief summary of the key steps, in what follows.

2.1. ALLFRAME

The input star list to ALLFRAME was generated by median averaging the 26 F555W and 8 F814W cosmic ray-split images of Table 1 to produce a cosmic ray-free frame for each chip. Iterative application of DAOPHOT and ALLSTAR led to the final master star list, which was input to ALLFRAME, and used to extract profile-fitting stellar photometry from the 34 individual frames. The adopted point spread functions (PSFs) were derived by one of us (PBS) from public domain *HST* WFPC2 observations of the globular clusters Pal 4 and NGC 2419.

Aperture photometry was performed on the 50 isolated bright stars listed in Table 2. DAOGROW was then employed to generate growth curves out to $0\farcs5$, allowing an aperture correction to be derived for each chip and filter, to ensure a match to the Holtzmann et al. (1995) photometric system. The photometric zero points, aperture corrections, and long exposure zero point correction were then used to finally convert from instrumental magnitudes to the standard system, following the procedure outlined in Hill et al. (1998).

EDITOR: PLACE TABLE 2 HERE.

2.2. DoPHOT

The DoPHOT philosophy concerning treatment of cosmic rays differs from that of ALLFRAME, in that each cosmic ray-split pair was first combined using a sigma detection algorithm which takes into account the problems of undersampling (Saha et al. 1996). The final calibration of DoPHOT magnitudes follows that outlined in Ferrarese et al. (1996) and Hill et al. (1998). Instrumental magnitudes were corrected to a $0\farcs5$ aperture magnitude using aperture corrections and zero points appropriate for long exposures, and converted to the standard system (Holtzmann et al. 1995). Calibrated DoPHOT photometry (and the associated error), for the 50 NGC 4725 reference stars, is listed in Table 2.

2.3. Comparison Between ALLFRAME and DoPHOT Photometry

A chip-by-chip comparison of ALLFRAME and DoPHOT photometry (both V- and I-bands) for the 50 reference stars of Table 2 is provided in Table 3. The agreement is very good for Chips 2-4 (i.e. , the WFC fields), with a mean difference of -0.01 ± 0.07 mag in V, and -0.03 ± 0.07 mag in I, being determined (in the sense of ALLFRAME-DoPHOT), well within 1σ of the internal errors. The largest difference found is -0.07 ± 0.07 mag in I for chip 4. Due to a complete absence of Cepheid candidates in Chip 1 (i.e. , the PC field), we will not concern ourselves with the obvious discrepancy therein between ALLFRAME and DoPHOT I-band photometry for the relevant 5 reference stars.

EDITOR: PLACE TABLE 3 HERE.

The comparison between ALLFRAME and DoPHOT mean magnitudes, for each of the 20 Cepheid candidates in common to each dataset (detailed in Section 3), is similarly presented in Table 3. The mean differences are $+0.057 \pm 0.091$ mag in V, and $+0.016 \pm 0.075$ mag in I, and manifest themselves in the slight offsets between the ALLFRAME and DoPHOT period-luminosity (PL) fits described in Section 4.

3. Cepheid Identification

In a similar vein to the philosophy of performing duel independent photometric reductions with ALLFRAME and DoPHOT, independent Cepheid identification techniques were employed by each reduction "team". Candidate Cepheids were extracted from the ALLFRAME dataset using TRIAL, Stetson's (1996) template light curve fitting algorithm, whereas a variant of Stellingwerf's (1978) phase dispersion minimization routine (Hughes 1989, and referred to as PDM henceforth) was adopted for the DoPHOT dataset.

Twenty-one high quality candidates were uncovered, the assigned identification numbers and coordinates (both (X,Y) on the respective WFC chip and (RA,DEC)) for which are listed in Table 4. The spatial distribution of the Cepheids in each chip is shown in Figure 2, with detailed ($4'' \times 4''$ windows centered upon each Cepheid) finding charts available in Figure 3.

EDITOR: PLACE TABLE 4 HERE.

EDITOR: PLACE FIGURE 2 HERE.

EDITOR: PLACE FIGURE 3 HERE.

The corresponding period and mean magnitude for each of the 21 Cepheids in question, as reported by TRIAL (for ALLFRAME data) and PDM (for DoPHOT data), is reproduced (along with their accompanying errors) in Table 5; ALLFRAME light curves for each, phased to their respective period, are presented in Figure 4 - V- and I-band photometry represented by solid dots and open squares, respectively. The tabulated epoch-by-epoch ALLFRAME photometry (and associated errors), for each of the 21 Cepheids, is given in Table 6.

EDITOR: PLACE TABLE 5 HERE.

EDITOR: PLACE FIGURE 4 HERE.

EDITOR: PLACE TABLE 6 HERE.

The 21 Cepheids listed in Table 5 have been identified in the deep V versus V-I color-magnitude diagram (CMD) of Figure 5. All but one of the Cepheids lie clearly in the instability strip; this outlyer (C14) is also (marginally) an outlyer in the V-band PL relation (Section 4).

EDITOR: PLACE FIGURE 5 HERE.

4. The Distance to NGC 4725

As described previously by Ferrarese et al. (1996), the apparent V- and I-band distance moduli (i.e. , μ_V and μ_I) to NGC 4725 are derived relative to that of the LMC, adopting Madore & Freedman's (1991) LMC PL relations, scaled to a true modulus of $\mu_\circ = 18.50 \pm 0.10$ mag and reddening E(V-I)=0.13. In fitting to the NGC 4725 Cepheid data (Table 5), the slope of the PL relations was fixed to those of Madore & Freedman's LMC PL relations.

The ALLFRAME/DoPHOT V- and I-band PL relations for NGC 4725 are shown in Figures 6/7. The open circle represents Cepheid candidate C14, which because of its marginal outlyer status (with respect to the instability strip) status in the CMD (Figure 5) and, to a lesser extent, in the V-band PL relation, was not included in the fit. The 20 Cepheids used in the final regression are denoted with solid circles, and listed in Table 5. The solid lines shown are the best fit regression, imposing the LMC PL slopes, while the dotted lines represent 1σ deviations from the mean of the LMC relations (i.e. , 0.27 mag in V, and 0.18 mag in I - Madore & Freedman 1991). The resulting apparent ALLFRAME distance moduli are $\mu_V = 31.00 \pm 0.06$ mag and $\mu_I = 30.80 \pm 0.06$ mag, with DoPHOT values of $\mu_V = 30.95 \pm 0.07$ mag and $\mu_I = 30.79 \pm 0.06$ mag. The derived reddenings are E(V-I)=0.21±0.02 (ALLFRAME) and E(V-I)=0.16±0.03 (DoPHOT). The 0.05 (0.01) mag offsets in the apparent ALLFRAME and DoPHOT V (I) band distance moduli are due to the 0.057 and 0.016 mag offsets in the Cepheid mean magnitudes, as noted previously in Section 2.3.

EDITOR: PLACE FIGURE 6 HERE.

EDITOR: PLACE FIGURE 7 HERE.

Adopting the Cardelli et al. (1989) extinction law, we derive true ALLFRAME and DoPHOT distance moduli of $\mu_{\circ} = 30.50 \pm 0.06$ mag and $\mu_{\circ} = 30.55 \pm 0.07$ mag, respectively, corresponding to $d = 12.6 \pm 0.4$ Mpc and $d = 12.9 \pm 0.4$ Mpc.

The errors listed above reflect internal errors alone, arising from scatter in the NGC 4725 PL relations. A more realistic assessment of the associated uncertainty, incorporating other potential random and systematic errors, is presented in Table 7. Uncertainties due to metallicity, LMC distance modulus, and photometric calibration all contribute to the NGC 4725 distance modulus error budget.

As in previous papers in this series (e.g. Hughes et al. 1998), the systematic uncertainty introduced by the adopted Cepheid PL calibration - ±0.12 mag (S1 in Table 7) - is dominated by the error in the LMC true modulus (±0.10 mag, from Madore & Freedman 1991). On the other hand, while such an uncertainty does encompass most LMC distance modulus predictions based upon Hipparcos trigonometric parallaxes of Galactic Cepheids (Feast & Catchpole 1997; Madore & Freedman 1998; Oudmaijer, Groenewegen & Schrijver 1998), Galactic subdwarfs (Gratton et al. 1997; Reid 1997), and the Barnes-Evans surface brightness technique applied to Galactic Cepheids (Gieren et al. 1998), it does *not* bracket any of the predictions based on RR Lyraes. The latter includes both direct Hipparcos proper motions (Fernley et al. 1998) and indirect statistical parallax of Galactic RR Lyraes (Layden et al. 1996; Popowski & Gould 1998a,b). Nor does it encompass recent independent distance determinations based upon the geometry of the SN 1987A ring

(Gould & Uza 1998[16]) or the luminosity of the red clump stars[17] (Udalski et al. 1998;

[16]Panagia's (1998) reinvestigation of the SN 1987A ring led to $\mu_o^{LMC} = 18.58 \pm 0.05$ mag, at odds with Gould & Uza's (1998) value of $\mu_o^{LMC} < 18.37$ mag (circular ring). The discrepancy can be traced to: (a) Panagia's assumption that the ring grew in extent by $\sim 6\%$ between 1988 and 1993 (Gould & Uza adopt the time-independent mean angular radius found by Plait et al. 1995 of 858 ± 11 mas, whereas Panagia attaches significant weight to the earlier pre-*HST* fix Jakobsen et al. 1991 value of $\sim 830 \pm 15$ mas (observed in 1988)). (b) Panagia derives a time for the onset of far side emission of 395 ± 5 days, whereas Gould & Uza, based upon the same Sonneborn et al. 1997 data, claim 378 ± 5 days. The different approaches to points (a) and (b) lead to the $\gtrsim 0.2$ mag offset in derived SN 1987A values for μ_o^{LMC}, and contribute (roughly) in equal measures. The ultimate resolution to this stalemate has yet to be reached.

[17]Both Udalski et al. (1998) and Stanek et al. (1998) claim $\mu_o^{LMC} \approx 18.08 \pm 0.15$, predicated upon the assumption that the mean absolute I magnitude of red clump stars in the LMC is identical to that of the solar neighborhood red clump, itself calibrated with accurate *Hipparcos* parallaxes - i.e. that age and metallicity effects in these differing stellar populations are of little importance. By employing the Seidel, Demarque & Weinberg (1987) theoretical red clump models, Cole (1998) recently demonstrated that neglect of such population effects can lead to an underestimate in the predicted μ_o^{LMC} of 0.28 mag. While intriguing, several caveats should be made concerning Cole's conclusion that $\mu_o^{LMC} = 18.36 \pm 0.17$ mag, and not the 18.08 ± 0.15 mag alluded to earlier: (a) In comparison with the red clump models of Lattanzio (1986) or VandenBerg (1985), the red clump luminosities from the Seidel et al. grid show the steepest dependence upon mass (i.e. age, in Cole's analysis), being $\sim 20\%$ greater than that predicted by Lattanzio, and a full factor of two greater than VandenBerg's models (for LMC metallicities). In practice, what this means, is that the 0.28 mag correction favoured by Cole, would be reduced to ~ 0.18 (using VandenBerg) or ~ 0.24 (using Lattanzio) - i.e. use of the Seidel et al. models maximizes the magnitude of this population effect correction. (b) More importantly perhaps, the Seidel et al. red clump models are evolved at constant helium abundance and core mass. Following Sweigart & Gross (1978), Cole demonstrates that the adoption of more realistic evolutionary scenarios would tend to decrease his predicted 0.28 mag correction by ~ 0.12 mag. Replicating Cole's analysis with modern self-consistent models such as Charbonnel et al. (1996) or Jimenez et al. (1998) are required. (c) From a purely empirical point of view, Stanek & Garnavich (1998) have shown that the stellar populations in three fields in M31 have identical absolute I-band magnitudes. Considering the galactocentric distances of the fields (6.7, 11.2, and 33.6 kpc) with Zaritsky et al.'s (1994) -0.018 dex/kpc abundance gradient, one would predict

Stanek, Zaritsky & Harris 1998). RR Lyrae, the SN 1987A ring, and LMC red clump stars, all favor a distance modulus of $\mu_o^{LMC} = 18.1 \rightarrow 18.4$ mag. Further assessment of these non-Cepheid-based LMC distances is obviously needed, as proof of their veracity (in lieu of Cepheid-based LMC distances) would imply an underestimate of the total systematic uncertainty in the PL calibration of Table 7 by up to a factor of three.[18]

The remaining systematic uncertainty in Table 7 which should be commented upon here is that due to a possible metallicity dependence of the Cepheid PL relation at V and I. Kennicutt et al. (1998a), based upon two fields in M101, find a metallicity dependence of the form $d\mu_o/d[O/H]$ = -0.24±0.16 mag/dex. If it can be shown that the NGC 4725 Cepheids differ substantially in metal abundance from those of the LMC Cepheids which calibrate the PL relation, a significant systematic error could be introduced into the derived distance.

Based upon 8 HII regions, Zaritsky et al. (1994) determined a mean oxygen abundance of $12 + \log(O/H) = 9.26 \pm 0.57$, at a galactocentric distance $r = 3$ kpc, with a corresponding abundance gradient of -0.022 ± 0.063 dex/kpc. With the WFPC2 fields at a galactocentric distance of $\sim 13 \pm 2$ kpc (recall the $10' \times 10'$ scale of Figure 1), we therefore estimate a mean oxygen abundance for the fields of $12 + \log(O/H) \approx 9.0 \pm 0.3$. In contrast, the mean calibrating LMC HII region abundance used by the *HST* Key Project is $12 + \log(O/H) = 8.5$ (Kennicutt et al. 1998a). Recalling the aforementioned Kennicutt et al. Cepheid metallicity

---

a metallicity differential of $\sim$ 0.5 dex, in agreement with indirect arguments based upon each field's CMD (Holland, Fahlman & Richer 1996; Rich et al. 1996). In the parlance of Cole, this 0.5 dex metallicity difference implies that there should be a 0.15 ± 0.05 mag difference in the absolute I-band magnitudes of the inner and outer M31 field CMDs. As Stanek & Garnavich show, such a magnitude difference is not observed, arguing against Cole's analysis. Obviously, further empirical checks are needed. Galactic open clusters of known age and metallicity will be particularly useful, to this end. To summarize, Cole's finding that the red clump technique leads to $\mu_o^{LMC} = 18.36 \pm 0.17$ mag, should be recast as $\mu_o^{LMC} = 18.36 \pm 0.17\,(+0.00/-0.22)$ mag, with the latter systematic uncertainty traced to points (a) and (b) elucidated upon above (note that both these systematic effects act in the same direction - i.e. reducing the magnitude of the claimed 0.28 mag correction).

[18]**Aside to the Team: If we really wanted to bracket all the feasible LMC μ_o^{LMC} values published in the past year, we would adopt $\mu_o^{LMC} = 18.4 \pm 0.3$ mag, instead of $\mu_o^{LMC} = 18.5 \pm 0.1$ mag! Such a systematic uncertainty, though, makes sorting out things like the LMC V and I PL zero points seem somewhat inconsequential! Just playing devil's advocate here ...**

dependence, this possible factor of three greater Cepheid metallicity in NGC 4725, in comparison with the LMC Cepheids, could cause the Cepheid distance modulus to NGC 4725 to be underestimated by $\sim 0.12 \pm 0.21$ mag. In keeping with earlier papers in this series, and noting the large uncertainty attached to the metallicity extrapolation for our Cepheid field, this potential correction to the distance modulus of $+0.12 \pm 0.21$ mag is not currently applied, but simply added to the appropriate systematic error budget in Table 7.

In light of the complete list of random and systematic errors shown in Table 7, our final quoted Cepheid-based true distance moduli to NGC 4725 are $\mu_o = 30.50 \pm 0.17$(random) $\pm$ 0.17(systematic) mag (ALLFRAME) and $\mu_o = 30.55 \pm 0.17$(random) $\pm$ 0.17(systematic) mag (DoPHOT), with reddenings of E(V-I)=0.21±0.02 (internal) and E(V-I)=0.16±0.03 (internal), respectively. The corresponding distances are 12.6 ± 1.0(random) $\pm$ 1.0(systematic) Mpc (ALLFRAME) and 12.9 ± 1.0(random) $\pm$ 1.0(systematic) Mpc (DoPHOT). We provide a complete list of Cepheid-derived galaxy distances in Table 9, updated to include our new determination for NGC 4725.

5. Previous Distance Determinations for NGC 4725 and the Coma I/II Groups

Previous distance determinations for NGC 4725 have been based upon either measurements of NGC 4725 itself, or indirectly through an assumed association with the Coma I or II Groups, within the Coma-Sculptor Cloud. Table 8 provides a summary of both families of distance determinations. The method employed is noted in column 1, the distance and quoted error (both in Mpc) in column 2, and the appropriate reference in column 3. We remind the reader that we are following the Group membership inventory listed in Table II of Tully (1988).

EDITOR: PLACE TABLE 8 HERE.

Early quoted values for NGC 4725 proper include Bottinelli et al.'s (1985) B-band Tully-Fisher (TF)-derived value of $d = 9.9 \pm 1.0$ Mpc and Tully's (1988) $d = 12.4$ Mpc, derived from assuming $H_o = 75$ km/s/Mpc, along with a simple Virgocentric flow model. Subsequent to this, and adopting an H-band TF relationship zero-point tied to M31, M33, and NGC 2403, Tully et al. (1992) found $d = 16.1$ Mpc.[19] Tully (1997) has since revised the TF distance to NGC 4725, by taking into account not only the H band, but also B-, R-, and I-bands, the average of which yields 12.6 ± 2.1 Mpc, in agreement with our Cepheid distance of 12.6 ± 1.0 Mpc.

Tonry et al. (1997) have recently derived an SBF distance to NGC 4725, assuming an association with NGCs 4494 and 4565 (strictly, Coma I group members in Tully's 1988 inventory), and taking the average as being representative. Their finding of 15.9 ± 0.6 Mpc is inconsistent with the Cepheid-derived distance to NGC 4725, at the $\sim 3\sigma$ level, although final revision of the SBF survey is still underway (Tonry 1998). The PNLF distances to NGCs 4494 and 4565 are 12.8 ± 0.9 Mpc and 10.5 ± 1.0 Mpc, respectively (Jacoby et al. 1996), in agreement with their corresponding GCLF distances — i.e. , Forbes (1996) finds 12.6 ± 0.9 Mpc, for NGC 4494, and Fleming et al. (1995) find 10.0 ± 1.5 Mpc, for NGC 4565. As it currently stands, the SBF distance to NGC 4725, and by association, NGCs 4494 and 4565, appears to be at odds with each of the Cepheid, PNLF, and GCLF distance indicators (see Section 5.1.2).

The GCLF distance to the Coma I Group member NGC 4278 is also in excellent agreement with our Cepheid distance to NGC 4725 (Forbes 1996); the PNLF distance to NGC 4278 is mildly discrepant, but only at the 2σ level. Finally, it is apparent that NGC 4414 lies significantly behind NGC 4725, with a Cepheid-derived distance of 19.1 ± 1.6 Mpc (Turner et al. 1998), making it of limited use for calibrating either Coma I or II Group secondary distance indicators.

5.1. Implications for Secondary Distance Indicators

5.1.1. Infrared Tully-Fisher Relationship

Our updated *interim* IRTF calibration, adopting Aaronson et al.'s (1982) H-band photometric index $H_{-0.5}$, and utilizing 19 of the calibrators listed in Table 9, is given by the initial entry to equation 1. For comparison, Freedman's (1990) earlier calibration, based upon only 5 local calibrators, is also listed in equation 1. The 0.46 magnitude offset between the two calibrations can be traced to the sample of five galaxies available to Freedman in 1990; *each* of these five (NGCs 224, 300, 598, 2403, and 3031) are $\sim 0.2 \rightarrow 0.5$ magnitudes

[19]Note, though, that the predicted distance output from their mass model of the same paper (Tully et al. 1992) was 20 Mpc, symptomatic of the well-documented "triple-value ambiguity", discussed therein.

fainter in $H_{-0.5}$ than expected for their HI linewidths. This only becomes apparent when the entire sample of 19 IRTF calibrators is considered.

$$\begin{aligned} H^{abs}_{-0.5} &= -21.48 - 10.13\,(\log \Delta V - 2.5) \qquad \text{(This Paper)} \qquad (1) \\ H^{abs}_{-0.5} &= -21.02 - 10.26\,(\log \Delta V - 2.5) \qquad \text{(Freedman 1990)} \end{aligned}$$

Equation 2 parallels that of equation 1, except Tormen & Burstein's (1995) revised H-band photometry (i.e. , H^{abs}_{g}) replaces that of Aaronson et al. (1982) (i.e. , $H^{abs}_{-0.5}$). Eighteen of the calibrators in Table 9 were adopted in deriving this *interim* calibration.

$$H^{abs}_{g} = -21.80 - 9.50\,(\log \Delta V - 2.5) \qquad \text{(This Paper)} \qquad (2)$$

Figure 8 summarizes graphically the IRTF calibrations of equations 1 and 2; the subject of this paper, NGC 4725, is clearly identified, possessing an H-band luminosity a factor of two lower than expected for its linewidth (similar to NGC 224≡M31).

EDITOR: PLACE FIGURE 8 HERE.

While we do not wish to belabor or overinterpret this mild divergence ($< 1\sigma$) from the mean Tully-Fisher relation, there are several points which should be made. It is apparent that NGC 4725 and its neighbor NCG 4747 (at a projected distance of $\sim$ 88 kpc) have undergone a past encounter. The striking $\sim$ 50 kpc-long HI plumes extending from the center of NGC 4747, including the one pointed directly at NGC 4725, clearly support this picture (Wevers et al. 1984). Given that NGC 4725 is twenty times as massive as NGC 4747, it is not surprising to find that while the latter is severly distorted, the former is far more stable against tidal interactions and only shows a minor elongation and possible warping of the outer south-eastern spiral arm. Still, a consequence of this distorted spiral arm is that the outer isophotes are less elongated than the inner ones, which may lead to an underestimate of the inclination should it be based solely on the outer isophotes. This may be source of the mild discrepancy between the photometric inclination of 46° (de Vaucouleurs et al. 1991) and the outer disk HI kinematical inclination of 53° (Wevers et al. 1984), although it should be stressed that the values are consistent within the quoted errors (±4°). We note in passing that increasing the assumed inclination from 46° to 53° will have the effect of shifting the $\log(\Delta V)$ for NGC 4725 in Figure 8 from 2.76 to 2.71, eliminating its $\sim 1\sigma$ outlyer status from the mean IRTF relation. Such issues will be addressed fully by Sakai et al. (1998); for the time being though, we choose to retain complete self-consistency with the compiled H-band magnitudes and 21cm linewidths in Tormen & Burstein (1995), as reflected in Table 9.

5.1.2. *Surface Brightness Fluctuations*

Besides its use as an IRTF calibrator, the bulge of NGC 4725 can be used as a calibrator for the SBF technique. As noted in Section 5, Tonry et al. (1997) derived the mean SBF distance to a Coma Cloud sub-group composed of NGCs 4494, 4565, and 4725, and found 15.9 ± 0.6 Mpc, approximately 3σ outside our Cepheid-derived NGC 4725 distance[20] (12.6 ± 1.0 Mpc).

The upper panel of Figure 9 compares Tonry et al.'s (1997) predicted SBF distances for the six groups/galaxies, outside the Local and M81 Groups,[21] which overlap with those listed in Table 9. The circled point represents our Cepheid distance to NGC 4725, and Tonry et al.'s Coma II SBF distance. The two Leo I galaxies (NGCs 3351 and 3368) have independently-derived Cepheid distances and are connected by a solid line, at the same SBF distance. Likewise, the five Virgo galaxies (NGCs 4321, 4536, 4548, 4571, and 4496A) and two Fornax (NGCs 1365 and 1425) galaxies are connected at their appropriate SBF distance.

EDITOR: PLACE FIGURE 9 HERE.

It is apparent that the SBF and Cepheid distances are in excellent agreement for 4/6 of the Tonry et al. (1997) groups shown in Figure 9; including NGCs 224 (Local Group) and 3031 (M81 Group) makes the agreement 6/8. The two deviants are NGCs 7331 and 4725; while the discrepancy in the case of the former *may* be lessened, to some degree, by the inclusion of an additional component of internal reddening to the bulge itself (Hughes et al. 1998), such an assumption for NGC 4725 would only increase the

---

[20]And, coincidentally, $\sim 3\sigma$ outside the Cepheid-derived NGC 4414 distance (19.1 ± 1.6 Mpc) of Turner et al. (1998).

[21]Tonry et al.'s (1997) Local Group and M81 Group SBF distances are in excellent agreement with the Cepheid-derived distances to NGCs 224 and 3031, respectively, but, for the sake of clarity, are not shown in Figure 9.

SBF-Cepheid distance discrepancy. Since the weighting in Tonry et al.'s Coma II distance is spread (approximately) equally between NGCs 4494, 4565, and 4725 (Tonry 1998), it might be tempting to target the SBF distances to the former two (elliptical) galaxies as suspect, and assume the SBF distance for NGC 4725 was correct. The problem then arises that the implied NGC 4494+4565 SBF distance ($\gtrsim$ 16 Mpc) would, recalling Table 8 (and anticipating the discussion of Section 5.1.3), be at odds with their PNLF and GCLF distances.[22] We are not in a position to resolve NGC 4725's SBF-Cepheid distance discrepancy here, so in lieu of further speculation, we feel the prudent approach for the time being would be to await the final calibration of Tonry et al.'s SBF Survey (Tonry 1998).

5.1.3. Planetary Nebula and Globular Cluster Luminosity Functions

Planetary nebula luminosity function (PNLF) and globular cluster luminosity function (GCLF) distances have been published for three galaxies in the Coma I Group - NGCs 4278, 4494, 4565. For the latter two, the PNLF and GCLF distances are in excellent agreement with each other (recall Table 8), although for NGC 4278 they are inconsistent at the $\sim 2\sigma$ level.

If we take Jacoby's (1997) unweighted mean distance modulus for Coma I, we find $\mu_o^{\rm PNLF} = 30.29 \pm 0.12$ mag, in comparison with our Coma II (i.e. NGC 4725) Cepheid distance of $\mu_o^{\rm Cep} = 30.50 \pm 0.17$ mag. The PNLF distance modulus is marginally smaller than the Cepheid one (although consistent within the errors), simply because NGCs 4278 and 4565 appear to lie $\sim$ 2 Mpc closer to us than NGC 4494. The latter's PNLF distance is virtually indistinguishable from our Cepheid distance to NGC 4725.

Taking Whitmore's (1997) compilation of GCLF distances for NGCs 4278 and 4494, supplemented with the Fleming et al. (1995) value for NGC 4565, we find an unweighted mean GCLF distance modulus for Coma I of $\mu_o^{\rm GCLF} = 30.37 \pm 0.15$ mag. Once again, the GCLF and Cepheid-derived distance moduli agree within their respective errors. Indeed, the agreement appears marginally better than for the PNLF-Cepheid comparison, simply

---

[22]**Aside to the Team: Tonry's individual SBF distances to NGCs 4494,4565, and 4725, are 15.8 ± 0.9, 16.6 ± 1.2, and 14.3 ± 2.2 Mpc, respectively, but he does <u>not</u> want them quoted individually, as he states unequivocally that he has no reason to suspect they are not at the same distance, SBF-wise, and does not want people making too much out of the individual SBF galactic distances. Note that his SBF distances to all three galaxies are at odds with the other secondary (and primary, in our case) distances.**

because Forbes' (1996) GCLF distance to NGC 4278 matches our Cepheid-derived value for NGC 4725 better than the Jacoby et al. (1996) PNLF value.

The middle and lower panels of Figure 9 provide a graphic comparison of PNLF and GCLF distances with those derived directly with Cepheids, for groups and clusters lying beyond the Local and M81 Groups. As for the SBF comparison of Section 5.1.2, the circled dot represents our new NGC 4725/Coma contribution.

6. Summary

HST WFPC2 imaging of the Coma II group galaxy NGC 4725 has led to the discovery of twenty Cepheids with periods ranging from ~14 to ~49 days. Based upon the resultant V- and I-band period-luminosity relations, we obtained true distance moduli of 30.50±0.17 (random)±0.17 (systematic) and 30.55±0.17 (random)±0.17 (systematic) mags, and reddenings of E(V-I)=0.21 ± 0.02 (internal) and 0.16 ± 0.03 (internal) mags, for the ALLFRAME- and DoPHOT-reduced datasets, respectively. The corresponding distances are then 12.6 ± 1.0 (random) ± 1.0 (systematic) and 12.9 ± 1.0 (random) ± 1.0 (systematic) Mpc, in excellent agreement with the most recent Tully-Fisher distance to NGC 4725 (Tully 1997). The Cepheid distance to NGC 4725 is also in good agreement with both the planetary nebula (Jacoby et al. 1996) and globular cluster luminosity function (Forbes 1996) distances to the Coma I Group elliptical NGC 4494, and indeed to the unweighted means of NGCs 4494, 4565, and 4278 (although the agreement is somewhat less satisfactory when comparing against the mean of the three Coma I members). The agreement between the Cepheid and surface brightness fluctuation distances is less satisfactory and remains unresolved at present.

The continued assistance of the NASA and STScI support staff, and in particular our program coordinator, Doug Van Orsow, is gratefully acknowledged. Support for this work was provided by NASA through grant GO-2227-87A from STScI. SMGH and PSB are grateful to NATO for travel support via a Collaborative Research Grant (960178). BKG wishes to thank John Tonry, Bill Harris, Robin Ciardullo, and Brent Tully, for several enlightening correspondences.

REFERENCES

Aaronson, M., et al. 1982, ApJS, 50, 241

Bottinelli, L., Gouguenheim, L., Paturel, G. & de Vaucouleurs, G. 1985, A&AS, 59, 43

Bottinelli, L., Gouguenheim, L., Paturel, G. & de Vaucouleurs, G. 1985, A&AS, 59, 43

Cardelli, J.A., Clayton, G.C. & Mathis, J.S. 1989, ApJ, 345, 245

Charbonnel, C., Meynet, G., Maeder, A. & Schaerer, D. 1996, A&AS, 115, 339

Cole, A.A. 1998, ApJ, in press (astro-ph/9804110)

de Vaucouleurs, G., de Vaucouleurs, A., Corwin, H., Buta, R., Paturel, A. & Fouqué, P. 1991, Third Reference Catalogue of Bright Galaxies (Berlin: Springer) ESA SP-310

Feast, M.W. & Catchpole, R.M. 1997, MNRAS, 286, L1

Fernley, J., Barnes, T.G., Skillen, I., Hawley, S.L., Hanley, C.J., Evans, D.W., Solano, E. & Garrido, R. 1998, A&A, 330, 515

Ferrarese, L., et al. 1996, ApJ, 464, 568

Ferrarese, L., et al. 1997, ApJ, 475, 853

Ferrarese, L., et al. 1998, ApJ, submitted

Fleming, D.E.B., Harris, W.E., Pritchet, C.J. & Danes, D.A. 1995, AJ, 109, 1044

Forbes, D.A. 1996, AJ, 112, 1409

Freedman, W.L. 1990, ApJ, 355, 35

Freedman, W.L., et al. 1994, ApJ, 435, L31

Gieren, W.P., Fouque, P. & Gomez, M. 1998, ApJ, 496, 17

Gould, A. & Uza, O. 1998, ApJ, 494, L118

Graham, J.A., et al. 1997, ApJ, 477, 535

Graham, J.A., et al. 1998a, ApJ, in preparation

Graham, J.A., et al. 1998b, unpublished

Gratton, R.G., Fusi Pecci, F., Carretta, E., Clementini, G., Corsi, C.E. & Lattanzi, M. 1997, ApJ, 491, 749

Hill, R.J., et al. 1998, ApJ, 496, 648

Holland, S., Fahlman, G.G. & Richer, H.B. 1996, AJ, 112, 1035

Holtzmann, J.A., et al. 1995, PASP, 107, 1065

Hughes, S.M.G. 1989, AJ, 97, 1634

Hughes, S.M.G., et al. 1998, ApJ, in press

Illingworth, G.D., et al. 1998, ApJ, in preparation

Jacoby, G.H. 1997, in Livio, M., Donahue, M. & Panagia, N., eds, The Extragalactic Distance Scale, Cambridge Univ Press, Cambridge, p. 197

Jacoby, G.H., Ciardullo, R. & Harris, W.E. 1996, ApJ, 462, 1

Jakobsen, P., et al. 1991, ApJ, 369, L63

Jimenez, R., Flynn, C. & Kotoneva, E. 1998, MNRAS, in press (astro-ph/9709056)

Kelson, D.D., et al. 1996, ApJ, 463, 26

Kennicutt, Jr., R.C., Freedman, W.L. & Mould, J.R. 1995, AJ, 110 1476

Kennicutt, Jr., R.C., et al. 1998a, ApJ, in press

Kennicutt, Jr., R.C., et al. 1998b, ApJ, in preparation

Lattanzio, J.C. 1986, ApJ, 311, 708

Layden, A.C., Hanson, R.B., Hawley, S.L., Klemola, A.R. & Hanley, C.J. 1996, AJ, 112, 2110

Macri, L.M., et al. 1998, ApJ, in preparation

Madore, B.F. & Freedman, W.L. 1991, PASP, 103, 933

Madore, B.F. & Freedman, W.L. 1998, ApJ, 492, 110

Madore, B.F., et al. 1998, ApJ, in preparation

Mould, J.R., Sakai, S., Hughes, S. & Han, M. 1997, in Livio, M., Donahue, M. & Panagia, N., eds, The Extragalactic Distance Scale, Cambridge Univ Press, Cambridge, p. 158

Mould, J.R., et al. 1998, ApJ, in preparation

Narasimha, D. & Mazumdar, A. 1998, ApJ, submitted (astro-ph/9803195)

Oudmaijer, R.D., Groenewegen, M.A.T. & Schrijver, H. 1998, MNRAS, 294, L41

Panagia, N. 1998, in Views on Distance Indicators, in press

Patat, F., Barbon, R., Cappellaro, E. & Turatto, M. 1994, A&A, 282, 731

Phelps, R.L., et al. 1998, ApJ, in press

Plait, P.C., Lundqvist, P., Chevalier, R.A. & Kirshner, R.P. 1995, ApJ, 439, 730

Popowski, P. & Gould, A. 1998a, ApJ, submitted (astro-ph/9703140)

Popowski, P. & Gould, A. 1998b, ApJ, submitted (astro-ph/9802168)

Rawson, D.M., et al. 1997, ApJ, 490, 517

Reid, I.N. 1997, AJ, 114, 161

Rich, R.M., Mighell, K.J., Freedman, W.L. & Neill, J.D. AJ, 111, 768

Saha, A., Labhardt, L., Schwengeler, H., Maccetto, F.D., Panagia, N., Sandage, A. & Tammann, G.A. 1994, ApJ, 425, 14

Saha, A., Sandage, A., Labhardt, L., Schwengeler, H., Tammann, G.A., Panagia, N. & Maccetto, F.D. 1995, ApJ, 438, 8

Saha, A., Sandage, A., Labhardt, L., Tammann, G.A., Maccetto, F.D. & Panagia, N. 1996a, ApJ, 466, 55

Saha, A., Sandage, A., Labhardt, L., Tammann, G.A., Maccetto, F.D. & Panagia, N. 1996b, ApJS, 107, 693

Saha, A., Sandage, A., Labhardt, L., Tammann, G.A., Maccetto, F.D. & Panagia, N. 1997, ApJ, 486, 1

Sakai, S., et al. 1998, ApJ, in preparation

Sandage, A. 1996, AJ, 111, 18

Sandage, A., et al. 1998, in preparation

Seidel, E., Demarque, P. & Weinberg, D. 1987, ApJS, 63, 917

Silbermann, N.A., et al. 1996, ApJ, 470 1

Silbermann, N.A., et al. 1998, ApJ, submitted

Simard, L. & Pritchet, C.J. 1994, AJ, 107, 503

Sonneborn, G., et al. 1997, ApJ, 477, 848

Stanek, K.Z. & Garnavich, P.M. 1998, ApJ, in press (astro-ph/9802121)

Stanek, K.Z., Zaritsky, D. & Harris, J. 1998, ApJ, submitted (astro-ph/9803181)

Stellingwerf, R.F. 1978, ApJ, 224, 953

Stetson, P.B. 1996, PASP, 108, 851

Stetson, P.B. 1994, AJ, 106, 205

Sweigart, A.V. & Gross, P.G. 1978, ApJS, 36, 405

Tanvir, N.R., Shanks, T., Ferguson, H.C. & Robinson, D.R.T. 1995, Nature, 377, 27

Tanvir, N.R., et al. 1998, in preparation

Tonry, J.L. 1998, priv comm

Tonry, J.L., Blakeslee, J.P., Ajhar, E.A. & Dressler, A. 1997, ApJ, 475, 399

Tormen, G. & Burstein, D. 1995, ApJS, 96, 123

Tully, R.B. 1997, priv comm

Tully, R.B. 1988, Nearby Galaxies Catalog (Cambridge: Cambridge University Press)

Tully, R.B. & Shaya, E.J. 1984, ApJ, 281, 31

Tully, R.B., Shaya, E.J. & Pierce, M.J. 1992, ApJS, 80, 479

Turner, A., et al. 1998, ApJ, submitted

Udalski, A., Szymański, M., Kubiak, M., Pietrzyński, G, Woźniak, P. & Zebruń, K. 1998, AcA, 48, 1

VandenBerg, D.A. 1985, ApJS, 58, 711

Wevers, B.M.H.R., Appleton, P.N., Davies, R.D. & Hart, L. 1984, A&A, 140, 125

Whitmore, B.C. 1997, in Livio, M., Donahue, M. & Panagia, N., eds, The Extragalactic Distance Scale, Cambridge Univ Press, Cambridge, p. 254

Zaritsky, D., Kennicutt, Jr., R.C. & Huchra, J.P. 1994, ApJ, 420, 87

Zaritsky, D., Smith, R., Frenk, C. & White, S.D.M. 1997, ApJ, 478, 39

Zepf, S.E., Newman, J., David, M., Freedman, W.L., Madore, B.F. & Silbermann, N.A. 1997, BAAS, 191, #03.07

This manuscript was prepared with the AAS LaTeX macros v4.0.

Fig. 1.— A $10' \times 10'$ ground-based image of NGC 4725, taken at the 2.5m Isaac Newton Telescope, by one of the authors (SMGH). North is to the top and east to the left. The WFPC2 footprint is superimposed, where C1 represents the Planetary Camera chip, and C2, C3, and C4 the Wide Field Camera chips.

Fig. 2.— (a) The $37'' \times 37''$ field of view of the PC (Chip 1) in NGC 4725. North is toward the bottom, east to the right. (b) The $80'' \times 80''$ field of view of the WFC Chip 2 in NGC 4725. North is toward the left, east to the bottom. Locations of the Cepheid candidates are marked, with detailed finding charts available for each in Figure 3. (c) The $80'' \times 80''$ field of view of the WFC Chip 3 in NGC 4725. North is toward the top, east to the left. Locations of the Cepheid candidates are marked, with detailed finding charts available for each in Figure 3. (d) The $80'' \times 80''$ field of view of the WFC Chip 4 in NGC 4725. North is toward the right, east to the top. Locations of the Cepheid candidates are marked, with detailed finding charts available for each in Figure 3.

Fig. 3.— Finder charts for each of the Cepheid candidates for NGC 4725. Each image is 41×41 pixels (i.e. , $4'' \times 4''$), with an orientation matching that of Figure 2.

Fig. 4.— Calibrated ALLFRAME V- (filled circles) and I-band (open squares) phased lightcurves (two cycles), for the Cepheids listed in Table 4.

Fig. 5.— Calibrated ALLFRAME photometry (V,V-I) color-magnitude diagram. The filled circles represent the 20 NGC 4725 Cepheid candidates of Table 4; the remaining candidate (C14) is denoted with an open circle, and was excluded from subsequent PL fitting due to its marginal outlyer status with respect to both the instability strip and the V-band PL relation (see Figures 6 and 7.

Fig. 6.— Period-luminosity relations in the V (top panel) and I (bottom panel) bands, based on the calibrated ALLFRAME photometry. The filled circles represent the 20 high-quality NGC 4725 Cepheid candidates found by TRIAL (see Tables 4 and 5), with the open circle representing (marginal) CMD outlyer C14. The solid lines are least squares fits, with the slope fixed to be that of the Madore & Freedman (1991) LMC PL-relations, while the dotted lines represent their corresponding 1σ dispersion. The inferred apparent distance moduli are then $\mu_V = 31.00 \pm 0.06$ mag (internal) and $\mu_I = 30.80 \pm 0.06$ mag (internal).

Fig. 7.— Period-luminosity relations in the V (top panel) and I (bottom panel) bands, based on the calibrated DoPHOT photometry. The filled circles represent the 18 high-quality NGC 4725 Cepheid candidates found by PDM (see Tables 4 and 5), with the open circle representing (marginal) CMD outlyer C14. The solid lines are least squares fits, with the slope fixed to be that of the Madore & Freedman (1991) LMC PL-relations, while the

dotted lines represent their corresponding 1σ dispersion. The inferred apparent distance moduli are then $\mu_V = 30.91 \pm 0.07$ mag (internal) and $\mu_I = 30.76 \pm 0.06$ mag (internal).

Fig. 8.— IRTF absolute calibration, with the upper panel showing absolute $H_{-0.5}$ magnitude versus HI linewidth log(ΔV), from the data in Table 9. Our interim calibration is represented by the solid curve, the least squares fit to the 19 galaxies in Table 9 with Cepheid-derived distances, HI linewidths, and $H_{-0.5}$ photometry - i.e. , $H^{abs}_{-0.5} = -21.48 - 10.13(\log \Delta V - 2.5)$. The dashed curve is Freedman's (1990) calibration, based upon 5 local calibrators - i.e. $H^{abs}_{-0.5} = -21.02 - 10.26(\log \Delta V - 2.5)$. The lower panel shows absolute H_g magnitudes versus log(ΔV), again, from the data in Table 9. Our interim calibration is represented by the solid curve, the least squares fit to the 18 galaxies in Table 9 with Cepheid-derived distances, HI linewidths, and H_g photometry - i.e. , $H_g = -21.80 - 9.50(\log \Delta V - 2.5)$. The circled dot, in both panels, represents NGC 4725.

Fig. 9.— Comparison of the predicted distance moduli from various secondary distance indicators with those determined directly with Cepheids, for galaxies lying beyond the Local and M81 Groups. The distance range shown is 8 $\rightarrow$ 20 Mpc. The upper, middle, and lower panels correspond to SBF, PNLF, and GCLF versus Cepheid distance, respectively. The labeled galaxy group/cluster designations follow Tonry et al. (1997), Jacoby (1997), and Whitmore (1997), for the SBF, PNLF, and GCLF comparisons, respectively. Cepheid distances to the N1023, Leo I, Coma I/II, N7331, Virgo, and Fornax Groups, are based upon NGC 925 (N1023), NGCs 3351 and 3368 (Leo I - connected by solid line), NGC 4725 (Coma I/II), NGC 7331 (N7331), NGCs 4321, 4536, 4548, 4571, and 4496A (Virgo), and NGCs 1365, 1425 (Fornax), respectively. The only *direct* comparison (i.e. , not influenced by an indirect assumption regarding (assumed) association with the Group in question) shown is that for NGC 3368 and the PNLF secondary distance indicator.

Table 1. HST Observations of NGC 4725

Epoch	Filename	Date	Julian Date	Exposure Times (s)		Filter
1	u2782j01t/2t	12/04/95	2449819.813	1500	1000	F555W
2	u2782k01t/2t	21/04/95	2449828.528	1500	1000	F555W
3	u2782l01t/2t	02/05/95	2449839.777	1500	1000	F555W
4	u2782m01t/2t	05/05/95	2449842.722	1500	1000	F555W
5	u2782n01t/2t	07/05/95	2449845.269	1500	1000	F555W
6	u2782o01t/2t	11/05/95	2449848.756	1500	1000	F555W
7	u2782p01t/2t	15/05/95	2449852.993	1500	1000	F555W
8	u2782q01t/2t	19/05/95	2449856.946	1500	1000	F555W
9	u2782r01p/2p	24/05/95	2449862.174	1500	1000	F555W
10	u2782s01p/2p	30/05/95	2449868.206	1500	1000	F555W
11	u2782t01t/2t	06/06/95	2449874.974	1500	1000	F555W
12	u2782u01t/2t	14/06/95	2449883.417	1500	1000	F555W
13	u2s76001t/2t	29/04/96	2450203.095	1100	1100	F555W
2	u2782k03t/4t	21/04/95	2449828.593	1000	1500	F814W
3	u2782l03t/4t	02/05/95	2449839.850	1000	1500	F814W
8	u2782q03t/4t	19/05/95	2449857.013	1000	1500	F814W
12	u2782u03t/4t	14/06/95	2449883.482	1000	1500	F814W
3	u2782l05t/6t	02/05/95	2449839.973	1500	1000	F439W
8	u2782q08t/9t	19/05/95	2449857.149	1300	1200	F439W
8	u2782q05t	19/05/95	2449857.082	230	...	F555W
8	u2782q06t	19/05/95	2449857.133	230	...	F814W
8	u2782q07t	19/05/95	2449857.138	230	...	F439W

Table 2—Continued

ID	Chip	X	Y	RA	Dec	ALLFRAME		DoPHOT	
				(J2000)		V	I	V	I
R42	4	636.5	373.0	12:50:39.99	25:33:42.2	24.07 ± 0.01	23.95 ± 0.04	24.15 ± 0.01	24.07 ± 0.06
R43	4	498.9	539.2	12:50:41.12	25:33:27.0	23.72 ± 0.02	23.66 ± 0.06	23.69 ± 0.02	23.74 ± 0.02
R44	4	162.8	525.8	12:50:40.78	25:32:53.8	23.77 ± 0.01	23.60 ± 0.02	23.84 ± 0.03	23.68 ± 0.03
R45	4	202.9	544.6	12:50:40.94	25:32:57.6	20.14 ± 0.01	17.14 ± 0.02	20.29 ± 0.05	17.13 ± 0.03
R46	4	365.6	546.0	12:50:41.07	25:33:13.7	24.33 ± 0.01	23.98 ± 0.04	24.41 ± 0.02	24.08 ± 0.05
R47	4	287.3	558.0	12:50:41.10	25:33:05.8	23.50 ± 0.01	23.06 ± 0.02	23.56 ± 0.02	23.13 ± 0.03
R48	4	296.4	665.3	12:50:41.90	25:33:05.7	24.46 ± 0.01	24.27 ± 0.04	24.50 ± 0.03	24.36 ± 0.08
R49	4	458.1	671.7	12:50:42.06	25:33:21.7	20.31 ± 0.00	18.76 ± 0.02	20.31 ± 0.03	18.86 ± 0.01
R50	4	305.0	699.0	12:50:42.15	25:33:06.2	22.62 ± 0.01	22.23 ± 0.02	22.59 ± 0.04	22.31 ± 0.03

Table 2—Continued

ID	Chip	X	Y	RA	Dec	ALLFRAME		DoPHOT	
				(J2000)		V	I	V	I
R42	4	636.5	373.0	12:50:39.99	25:33:42.2	24.07 ± 0.01	23.95 ± 0.04	24.15 ± 0.01	24.07 ± 0.06
R43	4	498.9	539.2	12:50:41.12	25:33:27.0	23.72 ± 0.02	23.66 ± 0.06	23.69 ± 0.02	23.74 ± 0.02
R44	4	162.8	525.8	12:50:40.78	25:32:53.8	23.77 ± 0.01	23.60 ± 0.02	23.84 ± 0.03	23.68 ± 0.03
R45	4	202.9	544.6	12:50:40.94	25:32:57.6	20.14 ± 0.01	17.14 ± 0.02	20.29 ± 0.05	17.13 ± 0.03
R46	4	365.6	546.0	12:50:41.07	25:33:13.7	24.33 ± 0.01	23.98 ± 0.04	24.41 ± 0.02	24.08 ± 0.05
R47	4	287.3	558.0	12:50:41.10	25:33:05.8	23.50 ± 0.01	23.06 ± 0.02	23.56 ± 0.02	23.13 ± 0.03
R48	4	296.4	665.3	12:50:41.90	25:33:05.7	24.46 ± 0.01	24.27 ± 0.04	24.50 ± 0.03	24.36 ± 0.08
R49	4	458.1	671.7	12:50:42.06	25:33:21.7	20.31 ± 0.00	18.76 ± 0.02	20.31 ± 0.03	18.86 ± 0.01
R50	4	305.0	699.0	12:50:42.15	25:33:06.2	22.62 ± 0.01	22.23 ± 0.02	22.59 ± 0.04	22.31 ± 0.03

Table 3. Comparison of ALLFRAME and DoPHOT Magnitudes

Chip	# Stars	ΔV^a	$\sigma_{\Delta V}$	ΔI^a	$\sigma_{\Delta I}$
		Reference Stars			
1	5	+0.002	0.071	-0.434	0.397
2	17	+0.022	0.073	+0.017	0.050
3	13	-0.045	0.038	-0.030	0.043
4	15	-0.020	0.063	-0.075	0.065
2-4	45	-0.011	0.068	-0.027	0.066
		Cepheids			
1	0	n/a	n/a	n/a	n/a
2	12	+0.088	0.097	+0.038	0.081
3	3[b]	-0.030	0.016	-0.060	0.029
4	5	+0.036	0.055	+0.006	0.042
2-4	20	+0.057	0.091	+0.016	0.075

[a]$\Delta \equiv$ALLFRAME-DoPHOT.

[b]Neglecting C14 of Table 5.

Table 4. Cepheid Candidates Detected in NGC 4725 - Coordinates

ID	Chip	X	Y	RA (J2000)	Dec (J2000)
C01	2	594.0	100.2	12:50:36.33	25:31:53.5
C02	2	570.6	226.2	12:50:35.42	25:31:56.9
C03	2	523.0	242.7	12:50:35.32	25:32:01.7
C04	2	629.5	336.9	12:50:34.57	25:31:51.9
C05	2	558.8	338.6	12:50:34.60	25:31:58.9
C06	2	675.2	358.3	12:50:34.38	25:31:47.5
C07	2	160.9	473.7	12:50:33.85	25:32:39.5
C08	2	90.3	521.5	12:50:33.54	25:32:46.9
C09	2	183.7	570.6	12:50:33.12	25:32:38.0
C10	2	566.3	585.3	12:50:32.78	25:32:00.2
C11	2	465.9	593.0	12:50:32.79	25:32:10.2
C12	2	97.3	655.6	12:50:32.55	25:32:47.3
C13	3	98.0	230.5	12:50:36.83	25:33:05.5
C14[a]	3	166.2	337.1	12:50:36.40	25:33:16.7
C15	3	353.9	420.4	12:50:35.08	25:33:26.5
C16	3	674.9	475.8	12:50:32.76	25:33:34.8
C17	4	133.9	230.6	12:50:38.59	25:32:53.8
C18	4	687.7	268.9	12:50:39.27	25:33:48.3
C19	4	724.1	287.8	12:50:39.43	25:33:51.7
C20	4	490.8	333.6	12:50:39.60	25:33:28.2
C21	4	705.9	408.3	12:50:40.30	25:33:48.8

[a]V-band PL relation outlyer; on, or near, main sequence, as opposed to instability strip.

Table 5. Cepheids Detected in NGC 4725 - Properties

ID	ALLFRAME/TRIAL			DoPHOT/PDM		
	Period (d)	V	I	Period (d)	V	I
C01	28.95 ± 0.05	25.43 ± 0.03	24.30 ± 0.06	26.9	25.37 ± 0.03	24.39 ± 0.13
C02	12.14 ± 0.02	26.45 ± 0.04	25.30 ± 0.07	12.3	26.25 ± 0.04	25.25 ± 0.07
C03	17.63 ± 0.04	26.01 ± 0.03	24.93 ± 0.05	17.6	25.94 ± 0.04	24.78 ± 0.06
C04	22.19 ± 0.09	25.87 ± 0.03	25.04 ± 0.04	22.2	25.81 ± 0.03	25.08 ± 0.07
C05	28.13 ± 0.28	26.14 ± 0.04	24.93 ± 0.06	29.8	25.91 ± 0.04	24.79 ± 0.05
C06	49.09 ± 0.25	24.86 ± 0.02	23.85 ± 0.03	49.7	24.84 ± 0.02	23.85 ± 0.05
C07	29.63 ± 0.08	25.78 ± 0.02	24.73 ± 0.05	29.4	25.84 ± 0.03	24.74 ± 0.07
C08	31.29 ± 0.45	25.44 ± 0.03	24.39 ± 0.04	33.9	25.44 ± 0.03	24.43 ± 0.05
C09	39.39 ± 0.06	24.85 ± 0.01	23.87 ± 0.02	38.7	24.69 ± 0.01	23.73 ± 0.03
C10	35.46 ± 0.43	24.81 ± 0.02	23.91 ± 0.04	38.1	24.81 ± 0.02	23.94 ± 0.05
C11	22.78 ± 0.02	25.70 ± 0.04	24.66 ± 0.05	22.5	25.44 ± 0.03	24.54 ± 0.05
C12	27.20 ± 0.11	25.87 ± 0.04	24.75 ± 0.06	29.5	25.82 ± 0.03	24.68 ± 0.05
C13	37.63 ± 0.17	25.49 ± 0.02	24.37 ± 0.03	35.8	25.54 ± 0.03	24.47 ± 0.04
C14[a]	15.53 ± 0.04	25.55 ± 0.02	25.08 ± 0.06	15.0	25.49 ± 0.02	24.92 ± 0.07
C15	17.62 ± 0.15	26.21 ± 0.04	25.22 ± 0.05	17.7	26.24 ± 0.04	25.25 ± 0.07
C16	14.20 ± 0.03	26.36 ± 0.03	25.35 ± 0.05	14.1	26.37 ± 0.04	25.40 ± 0.08
C17	35.93 ± 0.40	25.77 ± 0.02	24.68 ± 0.04	36.1	25.70 ± 0.03	24.66 ± 0.06
C18	31.03 ± 0.12	25.31 ± 0.02	24.23 ± 0.03	31.1	25.24 ± 0.02	24.29 ± 0.05
C19	28.93 ± 0.19	25.47 ± 0.02	24.43 ± 0.04	27.8	25.53 ± 0.02	24.45 ± 0.05
C20	48.41 ± 0.44	25.48 ± 0.02	24.28 ± 0.03	46.2	25.47 ± 0.03	24.22 ± 0.03
C21	13.90 ± 0.03	26.15 ± 0.04	25.36 ± 0.06	14.0	26.06 ± 0.04	25.33 ± 0.07

[a]V-band PL relation outlyer; on, or near, main sequence, as opposed to instability strip.

Table 6. Measured ALLFRAME Magnitudes and Standard Errors

HJD	Filter	magnitude	magnitude	magnitude	magnitude	magnitude	magnitude
		C01	C02	C03	C04	C05	C06
2449819.813	V	26.16 ± 0.18	27.00 ± 0.40	25.90 ± 0.11	25.68 ± 0.12	26.38 ± 0.22	24.95 ± 0.12
2449819.867	V	26.21 ± 0.17	26.42 ± 0.31	26.05 ± 0.19	25.61 ± 0.17	26.72 ± 0.37	24.99 ± 0.08
2449828.528	V	25.07 ± 0.05	25.65 ± 1.03	26.53 ± 0.19	26.50 ± 0.23	25.76 ± 0.06	25.18 ± 0.12
2449828.579	V	25.22 ± 0.14	25.77 ± 0.14	26.70 ± 0.38	26.29 ± 0.16	25.55 ± 0.13	25.13 ± 0.15
2449828.593	I	23.65 ± 0.41	25.04 ± 0.18	25.34 ± 0.30	25.26 ± 0.26	24.74 ± 0.16	24.11 ± 0.15
2449828.649	I	24.17 ± 0.24	25.12 ± 0.21	25.06 ± 0.19	25.37 ± 0.20	24.85 ± 0.14	23.95 ± 0.11
2449839.777	V	25.67 ± 0.09	26.45 ± 0.16	25.95 ± 0.12	25.60 ± 0.11	26.18 ± 0.20	23.65 ± 0.21
2449839.836	V	25.69 ± 0.19	26.41 ± 0.16	26.30 ± 0.22	25.44 ± 0.11	26.27 ± 0.39	25.07 ± 0.11
2449839.850	I	24.38 ± 0.10	25.95 ± 0.43	24.81 ± 0.17	24.82 ± 0.13	25.39 ± 0.31	23.81 ± 0.06
2449839.907	I	24.77 ± 0.16	25.17 ± 0.20	24.96 ± 0.13	24.98 ± 0.12	25.18 ± 0.27	24.07 ± 0.13
2449842.722	V	24.33 ± 0.44	26.17 ± 0.16	26.46 ± 0.21	25.61 ± 0.14	26.66 ± 0.27	24.81 ± 0.10
2449842.785	V	26.00 ± 0.14	26.25 ± 0.22	26.71 ± 0.35	25.88 ± 0.19	26.26 ± 0.23	24.82 ± 0.10
2449845.269	V	25.98 ± 0.17	26.68 ± 0.18	26.78 ± 0.22	26.05 ± 0.13	26.91 ± 0.30	24.41 ± 0.06
2449845.288	V	26.09 ± 0.20	26.77 ± 0.40	26.48 ± 0.32	26.05 ± 0.21	26.65 ± 0.35	24.59 ± 0.07
2449848.756	V	25.82 ± 0.08	27.23 ± 0.33	25.99 ± 0.12	26.06 ± 0.14	26.68 ± 0.32	24.43 ± 0.05
2449848.819	V	25.91 ± 0.15	27.34 ± 0.47	25.91 ± 0.17	26.01 ± 0.52	26.44 ± 0.33	24.43 ± 0.06
2449852.993	V	24.79 ± 0.07	25.74 ± 0.10	25.90 ± 0.10	24.10 ± 0.22	26.00 ± 0.13	24.62 ± 0.07
2449853.044	V	24.85 ± 0.09	23.29 ± 0.46	24.33 ± 0.65	26.74 ± 0.38	26.32 ± 0.27	23.58 ± 0.35
2449856.946	V	25.07 ± 0.07	26.98 ± 0.34	26.05 ± 0.18	25.82 ± 0.12	25.83 ± 0.15	24.67 ± 0.08
2449856.999	V	25.04 ± 0.10	26.37 ± 0.20	25.95 ± 0.23	25.82 ± 0.19	25.44 ± 0.12	24.81 ± 0.10
2449857.013	I	23.33 ± 0.81	25.41 ± 0.21	24.73 ± 0.12	24.82 ± 0.17	24.57 ± 0.19	23.72 ± 0.08
2449857.069	I	23.47 ± 0.46	25.26 ± 0.17	24.94 ± 0.17	25.15 ± 0.12	24.83 ± 0.13	23.76 ± 0.09
2449857.082	V	25.49 ± 0.25	25.96 ± 0.30	25.95 ± 0.40	26.59 ± 0.75	25.99 ± 0.51	24.76 ± 0.19
2449857.133	I	24.22 ± 0.21	...	24.65 ± 0.30	25.47 ± 0.75	24.35 ± 0.30	23.93 ± 0.18
2449862.174	V	25.43 ± 0.10	27.06 ± 0.35	26.71 ± 0.22	25.62 ± 0.10	25.84 ± 0.12	24.82 ± 0.09
2449862.233	V	24.98 ± 0.64	27.19 ± 0.50	26.42 ± 0.20	25.54 ± 0.10	26.09 ± 0.13	24.74 ± 0.10
2449868.206	V	25.80 ± 0.13	26.56 ± 0.21	25.38 ± 0.10	26.09 ± 0.12	25.48 ± 0.22	24.93 ± 0.08
2449868.264	V	25.78 ± 0.16	26.38 ± 0.23	25.51 ± 0.09	25.99 ± 0.19	25.58 ± 0.16	24.98 ± 0.09
2449874.974	V	26.06 ± 0.15	26.72 ± 0.18	25.78 ± 0.10	26.65 ± 0.33	26.67 ± 0.28	25.10 ± 0.06
2449875.025	V	26.08 ± 0.22	26.97 ± 0.48	26.24 ± 0.35	26.63 ± 0.30	26.67 ± 0.34	25.10 ± 0.10
2449883.417	V	25.00 ± 0.07	26.71 ± 0.17	26.05 ± 0.14	25.47 ± 0.07	25.73 ± 0.11	25.34 ± 0.11
2449883.468	V	24.87 ± 0.07	26.84 ± 0.27	26.41 ± 0.25	25.78 ± 0.20	25.79 ± 0.17	25.21 ± 0.12
2449883.482	I	24.16 ± 0.09	25.17 ± 0.24	24.95 ± 0.21	24.78 ± 0.15	24.78 ± 0.16	24.25 ± 0.11
2449883.538	I	23.86 ± 0.16	25.41 ± 0.22	25.30 ± 0.15	24.86 ± 0.10	24.54 ± 0.12	24.06 ± 0.28
2450203.095	V	24.97 ± 0.09	26.70 ± 0.33	25.47 ± 0.10	26.12 ± 0.17	26.11 ± 0.29	24.75 ± 0.06
2450203.109	V	24.93 ± 0.08	26.73 ± 0.27	25.42 ± 0.13	26.29 ± 0.16	26.20 ± 0.21	24.69 ± 0.06
		C07	C08	C09	C10	C11	C12
2449819.813	V	26.18 ± 0.11	25.64 ± 0.12	24.80 ± 0.06	25.36 ± 0.11	25.30 ± 0.09	26.14 ± 0.17
2449819.867	V	26.23 ± 0.22	25.56 ± 0.11	24.77 ± 0.06	25.44 ± 0.13	23.33 ± 0.27	25.99 ± 0.33
2449828.528	V	26.51 ± 0.19	25.98 ± 0.14	25.12 ± 0.08	24.44 ± 0.06	26.01 ± 0.21	25.47 ± 0.14

Table 6—Continued

HJD	Filter	magnitude	magnitude	magnitude	magnitude	magnitude	magnitude
2449828.579	V	26.92 ± 0.39	26.27 ± 0.23	25.23 ± 0.10	24.33 ± 0.31	26.27 ± 0.51	25.54 ± 0.14
2449828.593	I	25.22 ± 0.23	24.69 ± 0.16	23.97 ± 0.09	23.64 ± 0.13	24.83 ± 0.13	24.57 ± 0.11
2449828.649	I	25.06 ± 0.30	24.90 ± 0.16	23.88 ± 0.08	23.57 ± 0.05	25.05 ± 0.18	24.56 ± 0.13
2449839.777	V	25.66 ± 0.11	25.05 ± 0.08	25.16 ± 0.09	24.69 ± 0.08	25.03 ± 0.08	25.96 ± 0.17
2449839.836	V	25.56 ± 0.13	25.13 ± 0.08	25.18 ± 0.08	24.91 ± 0.12	25.21 ± 0.10	26.41 ± 0.38
2449839.850	I	24.50 ± 0.13	24.27 ± 0.10	24.09 ± 0.10	23.78 ± 0.10	24.54 ± 0.17	22.93 ± 0.34
2449839.907	I	24.62 ± 0.11	24.14 ± 0.07	24.17 ± 0.11	23.79 ± 0.09	24.35 ± 0.09	24.82 ± 0.13
2449842.722	V	25.69 ± 0.13	25.27 ± 0.08	24.78 ± 0.07	25.04 ± 0.10	24.39 ± 0.27	26.66 ± 0.21
2449842.785	V	25.77 ± 0.14	25.31 ± 0.11	24.76 ± 0.09	24.99 ± 0.12	25.38 ± 0.14	26.43 ± 0.29
2449845.269	V	25.70 ± 0.10	24.83 ± 0.33	24.38 ± 0.05	24.91 ± 0.07	25.54 ± 0.08	26.29 ± 0.22
2449845.288	V	25.23 ± 1.11	25.51 ± 0.17	24.41 ± 0.06	24.88 ± 0.07	25.65 ± 0.13	26.36 ± 0.30
2449848.756	V	26.19 ± 0.14	25.59 ± 0.10	24.44 ± 0.06	25.04 ± 0.10	25.95 ± 0.13	26.14 ± 0.17
2449848.819	V	26.06 ± 0.17	25.57 ± 0.09	24.47 ± 0.08	24.91 ± 0.09	25.66 ± 0.13	26.17 ± 0.29
2449852.993	V	26.64 ± 0.22	24.09 ± 0.26	24.61 ± 0.06	25.12 ± 0.11	25.39 ± 0.73	24.22 ± 0.60
2449853.044	V	26.52 ± 0.15	25.77 ± 0.29	24.75 ± 0.08	25.35 ± 0.14	25.96 ± 0.17	25.47 ± 0.09
2449856.946	V	26.27 ± 0.21	25.92 ± 0.22	24.82 ± 0.06	25.37 ± 0.12	26.28 ± 0.17	25.59 ± 0.16
2449856.999	V	26.38 ± 0.26	26.24 ± 0.18	24.71 ± 0.09	25.36 ± 0.14	25.90 ± 0.21	25.60 ± 0.15
2449857.013	I	25.06 ± 0.39	24.74 ± 0.12	23.77 ± 0.06	24.46 ± 0.16	24.70 ± 0.14	24.82 ± 0.17
2449857.069	I	25.24 ± 0.23	25.00 ± 0.18	23.76 ± 0.08	24.29 ± 0.11	24.52 ± 0.34	24.56 ± 0.14
2449857.082	V	25.89 ± 0.41	26.77 ± 0.95	24.64 ± 0.18	25.28 ± 0.34	26.62 ± 1.05	25.60 ± 0.24
2449857.133	I	24.81 ± 0.30	24.78 ± 0.49	23.79 ± 0.16	24.50 ± 0.31	26.53 ± 0.78	25.05 ± 0.28
2449862.174	V	25.46 ± 0.11	25.88 ± 0.13	24.88 ± 0.05	24.76 ± 0.14	25.17 ± 0.12	25.97 ± 0.13
2449862.233	V	25.34 ± 0.11	25.98 ± 0.18	24.79 ± 0.08	24.73 ± 0.06	25.07 ± 0.09	25.94 ± 0.16
2449868.206	V	25.40 ± 0.09	24.83 ± 0.06	25.18 ± 0.09	24.42 ± 0.04	25.70 ± 0.07	23.55 ± 0.24
2449868.264	V	25.40 ± 0.22	24.74 ± 0.08	25.11 ± 0.11	24.46 ± 0.05	25.55 ± 0.12	26.31 ± 0.24
2449874.974	V	26.02 ± 0.13	25.18 ± 0.09	25.45 ± 0.08	24.67 ± 0.08	26.22 ± 0.13	26.31 ± 0.17
2449875.025	V	25.83 ± 0.17	25.11 ± 0.14	25.56 ± 0.11	24.65 ± 0.05	26.23 ± 0.23	25.79 ± 0.15
2449883.417	V	26.40 ± 0.22	25.75 ± 0.13	24.48 ± 0.06	24.94 ± 0.10	25.14 ± 0.49	25.49 ± 0.13
2449883.468	V	26.27 ± 0.16	25.36 ± 0.20	24.58 ± 0.08	25.05 ± 0.15	25.58 ± 0.13	25.59 ± 0.14
2449883.482	I	25.17 ± 0.19	24.56 ± 0.12	23.71 ± 0.06	23.95 ± 0.11	24.55 ± 0.10	24.42 ± 0.13
2449883.538	I	24.99 ± 0.19	24.43 ± 0.15	23.69 ± 0.06	22.87 ± 0.42	24.66 ± 0.09	24.81 ± 0.14
2450203.095	V	26.22 ± 0.20	26.04 ± 0.17	24.40 ± 0.05	25.30 ± 0.13	25.35 ± 0.09	25.93 ± 0.20
2450203.109	V	25.98 ± 0.15	26.12 ± 0.19	24.40 ± 0.08	25.06 ± 0.15	25.24 ± 0.08	26.44 ± 0.25
		C13	C14	C15	C16	C17	C18
2449819.813	V	25.35 ± 0.39	25.56 ± 0.11	26.14 ± 0.33	26.67 ± 0.29	25.19 ± 0.07	25.47 ± 0.12
2449819.867	V	25.62 ± 0.17	25.52 ± 0.10	26.15 ± 0.24	26.79 ± 0.38	25.33 ± 0.10	25.68 ± 0.18
2449828.528	V	25.71 ± 0.14	25.42 ± 0.08	26.35 ± 0.20	25.95 ± 0.16	25.73 ± 0.11	26.04 ± 0.20
2449828.579	V	25.84 ± 0.17	25.16 ± 0.08	23.33 ± 0.56	25.98 ± 0.16	25.83 ± 0.17	25.88 ± 0.11
2449828.593	I	24.69 ± 0.18	24.95 ± 0.12	25.64 ± 0.27	25.05 ± 0.20	24.57 ± 0.19	24.67 ± 0.12
2449828.649	I	24.71 ± 0.11	24.91 ± 0.14	25.57 ± 0.21	25.12 ± 0.14	24.38 ± 0.15	24.70 ± 0.08
2449839.777	V	25.18 ± 0.10	25.77 ± 0.13	25.82 ± 0.14	26.42 ± 0.15	26.08 ± 0.09	24.89 ± 0.07

Table 6—Continued

HJD	Filter	magnitude	magnitude	magnitude	magnitude	magnitude	magnitude
2449839.836	V	25.24 ± 0.11	25.90 ± 0.14	25.55 ± 0.11	26.49 ± 0.22	26.20 ± 0.18	24.93 ± 0.09
2449839.850	I	24.25 ± 0.09	25.53 ± 0.25	24.91 ± 0.12	25.17 ± 0.18	24.93 ± 0.17	23.99 ± 0.10
2449839.907	I	24.41 ± 0.09	25.32 ± 0.30	24.88 ± 0.12	25.44 ± 0.25	24.70 ± 0.12	24.01 ± 0.08
2449842.722	V	25.14 ± 0.08	25.63 ± 0.10	26.00 ± 0.16	25.88 ± 0.14	26.14 ± 0.13	25.12 ± 0.08
2449842.785	V	25.02 ± 0.09	25.78 ± 0.15	25.88 ± 0.13	25.58 ± 0.10	26.22 ± 0.25	25.12 ± 0.09
2449845.269	V	25.21 ± 0.10	25.31 ± 0.07	26.28 ± 0.15	26.30 ± 0.14	25.95 ± 0.16	25.21 ± 0.08
2449845.288	V	25.07 ± 0.11	25.32 ± 0.13	26.41 ± 0.40	26.20 ± 0.19	26.34 ± 0.24	25.14 ± 0.11
2449848.756	V	25.40 ± 0.11	25.47 ± 0.08	26.57 ± 0.16	26.60 ± 0.20	26.09 ± 0.16	25.40 ± 0.08
2449848.819	V	25.30 ± 0.05	25.42 ± 0.13	26.99 ± 0.38	27.21 ± 0.40	26.01 ± 0.22	25.43 ± 0.13
2449852.993	V	25.51 ± 0.09	25.72 ± 0.10	26.66 ± 0.29	26.63 ± 0.22	25.52 ± 0.13	25.71 ± 0.09
2449853.044	V	25.60 ± 0.15	25.67 ± 0.13	26.36 ± 0.21	26.83 ± 0.33	25.47 ± 0.10	24.64 ± 0.40
2449856.946	V	25.58 ± 0.15	25.76 ± 0.10	25.53 ± 0.11	26.06 ± 0.16	25.41 ± 0.09	25.80 ± 0.09
2449856.999	V	25.61 ± 0.14	25.51 ± 0.12	25.70 ± 0.13	25.84 ± 0.14	25.38 ± 0.09	25.69 ± 0.15
2449857.013	I	24.29 ± 0.11	25.39 ± 0.29	24.84 ± 0.16	25.00 ± 0.21	24.39 ± 0.14	24.48 ± 0.09
2449857.069	I	24.38 ± 0.11	21.61 ± 0.36	24.94 ± 0.14	25.41 ± 0.16	24.51 ± 0.08	24.56 ± 0.09
2449857.082	V	25.65 ± 0.33	25.83 ± 0.36	25.99 ± 0.46	25.85 ± 0.41	25.21 ± 0.13	21.94 ± 0.36
2449857.133	I	24.67 ± 0.42	25.91 ± 0.89	25.32 ± 0.57	24.92 ± 0.35	25.23 ± 0.74	24.91 ± 0.32
2449862.174	V	25.75 ± 0.14	25.36 ± 0.08	26.42 ± 0.18	26.66 ± 0.32	25.51 ± 0.09	25.72 ± 0.09
2449862.233	V	25.78 ± 0.17	25.40 ± 0.12	26.28 ± 0.28	26.77 ± 0.34	25.56 ± 0.12	25.75 ± 0.70
2449868.206	V	25.85 ± 0.15	25.83 ± 0.13	26.67 ± 0.56	26.59 ± 0.15	25.86 ± 0.14	24.64 ± 0.07
2449868.264	V	25.85 ± 0.16	25.69 ± 0.14	26.77 ± 0.30	26.51 ± 0.24	25.56 ± 0.29	24.70 ± 0.07
2449874.974	V	25.47 ± 0.13	25.41 ± 0.10	25.71 ± 0.12	26.42 ± 0.25	26.14 ± 0.14	25.11 ± 0.08
2449875.025	V	25.47 ± 0.15	25.31 ± 0.10	25.75 ± 0.13	26.25 ± 0.20	26.14 ± 0.14	25.16 ± 0.08
2449883.417	V	25.05 ± 0.57	25.84 ± 0.12	25.97 ± 0.47	26.10 ± 0.14	26.12 ± 0.17	25.59 ± 0.11
2449883.468	V	25.22 ± 0.09	25.67 ± 0.11	26.92 ± 0.27	26.20 ± 0.22	26.06 ± 0.22	25.59 ± 0.13
2449883.482	I	24.07 ± 0.08	25.38 ± 0.33	25.26 ± 0.35	25.64 ± 0.33	25.19 ± 0.22	24.36 ± 0.09
2449883.538	I	24.18 ± 0.09	24.65 ± 0.58	25.42 ± 0.20	25.19 ± 0.21	25.31 ± 0.18	23.07 ± 0.31
2450203.095	V	25.79 ± 0.11	25.40 ± 0.17	26.62 ± 0.38	26.53 ± 0.22	26.23 ± 0.16	25.88 ± 0.14
2450203.109	V	25.69 ± 0.12	25.27 ± 0.09	27.22 ± 0.37	26.96 ± 0.28	26.27 ± 0.25	25.75 ± 0.12
		C19	C20	C21			
2449819.813	V	25.82 ± 0.11	25.35 ± 0.08	26.47 ± 0.18			
2449819.867	V	25.92 ± 0.18	25.32 ± 0.10	26.93 ± 0.39			
2449828.528	V	25.96 ± 0.10	25.57 ± 0.08	26.08 ± 0.11			
2449828.579	V	25.04 ± 0.89	25.55 ± 0.16	26.13 ± 0.19			
2449828.593	I	24.77 ± 0.69	22.99 ± 0.34	25.06 ± 0.16			
2449828.649	I	24.95 ± 0.10	24.30 ± 0.06	25.48 ± 0.19			
2449839.777	V	25.27 ± 0.10	25.76 ± 0.14	25.78 ± 0.15			
2449839.836	V	25.38 ± 0.22	25.58 ± 0.12	25.84 ± 0.14			
2449839.850	I	24.34 ± 0.12	24.32 ± 0.13	25.27 ± 0.21			
2449839.907	I	24.21 ± 0.05	24.29 ± 0.09	25.47 ± 0.21			
2449842.722	V	25.76 ± 0.08	25.90 ± 0.14	26.35 ± 0.17			

Table 6—Continued

HJD	Filter	magnitude	magnitude	magnitude	magnitude	magnitude	magnitude
2449842.785	V	25.60 ± 0.14	25.76 ± 0.15	26.12 ± 0.20			
2449845.269	V	25.80 ± 0.12	25.77 ± 0.16	26.44 ± 0.13			
2449845.288	V	25.56 ± 0.07	25.77 ± 0.18	26.50 ± 0.22			
2449848.756	V	26.00 ± 0.14	25.67 ± 0.14	26.58 ± 0.19			
2449848.819	V	25.42 ± 0.35	25.43 ± 0.10	26.84 ± 0.28			
2449852.993	V	26.02 ± 0.17	25.43 ± 0.13	25.50 ± 0.09			
2449853.044	V	25.86 ± 0.10	25.53 ± 0.11	25.59 ± 0.11			
2449856.946	V	25.93 ± 0.08	25.27 ± 0.07	26.16 ± 0.11			
2449856.999	V	26.29 ± 0.19	24.09 ± 0.45	25.91 ± 0.15			
2449857.013	I	24.75 ± 0.13	24.18 ± 0.07	25.25 ± 0.19			
2449857.069	I	24.72 ± 0.18	24.15 ± 0.07	25.22 ± 0.14			
2449857.082	V	25.81 ± 0.41	25.92 ± 0.41	26.60 ± 0.53			
2449857.133	I	25.27 ± 0.45	24.32 ± 0.17	26.06 ± 1.41			
2449862.174	V	24.84 ± 0.06	25.26 ± 0.08	26.65 ± 0.19			
2449862.233	V	24.80 ± 0.07	25.16 ± 0.08	26.58 ± 0.24			
2449868.206	V	25.30 ± 0.08	25.30 ± 0.10	25.85 ± 0.11			
2449868.264	V	25.29 ± 0.09	25.45 ± 0.14	26.02 ± 0.13			
2449874.974	V	25.60 ± 0.12	25.53 ± 0.11	26.40 ± 0.23			
2449875.025	V	25.69 ± 0.10	25.36 ± 0.11	26.81 ± 0.47			
2449883.417	V	26.02 ± 0.13	25.66 ± 0.11	26.03 ± 0.13			
2449883.468	V	25.73 ± 0.12	25.59 ± 0.16	26.29 ± 0.16			
2449883.482	I	24.65 ± 0.13	24.32 ± 0.10	25.09 ± 0.19			
2449883.538	I	24.81 ± 0.10	24.42 ± 0.08	25.21 ± 0.22			
2450203.095	V	26.00 ± 0.14	25.30 ± 0.10	23.73 ± 0.52			
2450203.109	V	26.15 ± 0.24	25.36 ± 0.10	26.04 ± 0.14			

Table 7. ALLFRAME Error Budget

	Source of Uncertainty	Error (mag)	Notes
CEPHEID PL CALIBRATION			
(a)	LMC True Modulus	±0.10	(1)
(b)	V PL Zero Point	±0.05	(2),(3)
(c)	I PL Zero Point	±0.03	(2),(4)
(S1)	PL Systematic Uncertainty	±0.12	(a),(b),(c) combined in quadrature
NGC 4725 MODULUS			
(d)	HST V-Band Zero Point	±0.05	(5)
(e)	HST I-Band Zero Point	±0.05	(5)
(R1)	Cepheid True Modulus	±0.15	(6)
(f)	PL Fit (V)	±0.06	(7)
(g)	PL Fit (I)	±0.06	(7)
(R2)	Cepheid True Modulus	±0.08	(f),(g) partially correlated,(8)
(S2)	Metallicity Uncertainty	$+0.12 \pm 0.21$	See text for details
TOTAL UNCERTAINTY			
(R)	Random Errors	±0.17	(R1),(R2) combined in quadrature
(S)	Systematic Errors	±0.17	(S1),(S2) combined in quadrature

(1) Adopted from Madore & Freedman (1991). (2) Derived from the observed scatter in the Madore & Freedman (1991) PL relation, with 32 contributing Cepheids. (3) V-band 1σ scatter: ±0.27 mag. (4) I-band 1σ scatter: ±0.18 mag. (5) Contributing uncertainties from aperture corrections, the Holtzmann et al. (1995) zero points, and the long versus short uncertainty, combined in quadrature. Adopted aperture correction contribution is the worst-case formal uncertainty (±0.04 mag) for the NGC 4725 aperture corrections. Adopted Holtzmann et al. zero point uncertainty is ±0.02 mag. Adopted long versus short exposure correction uncertainty is ±0.02 mag. (6) Assuming that photometric errors (d,e) are uncorrelated between filters, and noting that that V and I magnitudes are multiplied by +1.45 and -2.45, respectively, when correcting for reddening, results in a derived error on the true modulus of $[(1.45)^2(0.05)^2 + (-2.45)^2(0.05)^2]^{1/2} = 0.15$ mag. (7) Uncertainties for the mean apparent V and I moduli are limited by the apparent width of the derived PL relation, reduced by the population size of contributing Cepheids for NGC 4725 (20 variables). Contributing effects include photometric errors, differential reddening, and intrinsic strip filling. (8) The partially correlated nature of the derived PL width uncertainties is taken into account by the (correlated) dereddening procedure, coupled with the largely "degenerate-with-reddening" positioning of individual Cepheids within the instability strip.

Table 8. Published Distances to NGC 4725 and the Coma Cloud[a]

Method	Distance (Mpc)	Reference
	NGC 4725 (Coma II)	
TF (B-band)	9.9 ± 1.0	Bottinelli et al. (1985)
Mass Model	12.4	Tully (1988)
TF (H-band)	16.1	Tully et al. (1992)
Mass Model	20	Tully et al. (1992)
TF (BRIH-band)	12.6 ± 2.1	Tully (1997)
Cepheids	12.6 ± 1.0	This paper (ALLFRAME)
	NGC 4414 (Coma I)	
Cepheids	19.1 ± 1.6	Turner et al. (1998)
	NGC 4278 (Coma I)	
GCLF[b]	13.2 ± 0.9	Forbes (1996)
PNLF	10.2 ± 1.0	Jacoby et al. (1996)
	NGC 4494 (Coma I)	
Mass Model	11.7	Tully & Shaya (1984)
SBF	15.0 ± 2.3	Simard & Pritchet (1994)
GCLF[b]	14.5 ± 2.9	Fleming et al. (1995)
GCLF[b]	12.6 ± 0.9	Forbes (1996)
PNLF	12.8 ± 0.9	Jacoby et al. (1996)
	NGC 4565 (Coma I)	
Mass Model	11.0	Tully & Shaya (1984)
SBF	10.4 ± 0.4	Simard & Pritchet (1994)
GCLF[b]	10.0 ± 1.5	Fleming et al. (1995)
PNLF	10.5 ± 1.0	Jacoby et al. (1996)
	Average of NGCs 4150,4251,4283 (Coma I)	
SBF	15.5 ± 0.6	Tonry et al. (1997)
	Average of NGCs 4494,4565 (Coma I) and NGC 4725 (Coma II)	
SBF[c]	15.9 ± 0.6	Tonry et al. (1997)

[a]Coma I and Coma II Group membership is that listed in Tully (1988) - i.e. , Groups 14-1 and 14-2, respectively, from his Table II.

[b]Fleming et al.'s (1995) results are based upon ground-based CFHT data, whereas Forbes (1996) used HST. The latter reference revisits Fleming et al.'s conclusions, in light of the HST results.

[c]Tonry et al. (1997) compute a Coma II Group distance based upon the (approximate) mean of the SBF distances to NGCs 4494, 4565, and 4725 (Tonry 1998). Tully's (1988) inventory would place NGCs 4494 and 4565 in the Coma I Group, with only NGC 4725 *strictly* a Coma II Group member.

Table 9. Galaxies with Cepheid-Derived Distances[a]

Galaxy	DM	log ΔV	$H_{-0.5}$	H_g	Distance Reference
NGC 224	24.40	2.751	0.91	0.47	Freedman (1990)
NGC 300	26.67	2.371[b]	7.00[b]	–	Madore & Freedman (1991)
NGC 598	24.50	2.392	4.38	4.00	Freedman (1990)
NGC 925	29.84	2.422	8.74	8.36	Silbermann et al. (1996)
NGC 1326A	Cyc 6	2.608	8.16	8.11	Kennicutt et al. (1998b)
NGC 1365	31.27	2.673	7.20	6.84	Silbermann et al. (1998)
NGC 1425	Cyc 6	2.606	8.88	8.73	Mould et al. (1998)
NGC 2090	30.41	2.529	8.62	8.47	Phelps et al. (1998)
NGC 2403	27.51	2.488	6.45	6.21	Madore & Freedman (1991)
NGC 2541	30.47	2.384	10.30	10.22	Ferrarese et al. (1998)
NGC 3031	27.80	2.716	4.38	4.18	Freedman et al. (1994)
NGC 3109	25.94	–	–	–	Madore & Freedman (1991)
NGC 3198	Cyc 5	2.535	8.71	8.53	Illingworth et al. (1998)
NGC 3319	Cyc 6	2.428	10.40	10.39	Madore et al. (1998)
NGC 3351	30.01	2.573[c]	7.41[c]	7.29	Graham et al. (1997)
NGC 3368	29.91	2.709[c]	6.87[c]	6.72	Graham et al. (1998b)
NGC 3368	30.32	2.709[c]	6.87[c]	6.72	Tanvir et al. (1995)
NGC 3377A	Cyc 5	–	–	–	Tanvir et al. (1998)
NGC 3621	29.20	2.536	7.40	6.70	Rawson et al. (1997)
NGC 3627	Cyc 6	2.618	6.70	6.55	Sandage et al. (1998)
NGC 4321	31.04	–	–	7.80	Ferrarese et al. (1997)
NGC 4321	31.55	–	–	7.80	Narasimha & Mazumdar (1998)
NGC 4414	31.41	2.697	7.83	7.74	Turner et al. (1998)
NGC 4496A	31.13	–	–	–	Saha et al. (1996b)
NGC 4535	31.02	2.618	8.45	8.58	Macri et al. (1998)
NGC 4536	31.10	2.576	8.30	8.11	Saha et al. (1996a)
NGC 4548	Cyc 6	–	–	–	Graham et al. (1998a)
NGC 4571	30.87	–	–	–	Pierce et al. (1994)
"	Cyc 6	–	–	–	Pierce et al. (1998)
NGC 4603	Cyc 6	2.761	9.32	9.26	Zepf et al. (1997)
NGC 4639	32.03	–	–	–	Saha et al. (1997)
NGC 4725	30.50	2.759	7.06	7.03	This paper
IC 4182	28.36	–	–	–	Saha et al. (1994)
NGC 5253	28.10	–	–	8.78	Saha et al. (1995)
NGC 5457	29.34	–	–	6.35	Kelson et al. (1996)
NGC 7331	30.92	2.740	6.44	6.08	Hughes et al. (1998)

[a]HI linewidths and H-band magnitudes from the compilation of Tormen & Burstein (1995), except where noted. Where independent ALLFRAME and DoPHOT-based Cepheid distances exist, the tabulated distance modulus in column 2 reflects the former.

[b]Freedman (1990)

[c]Mould et al. (1997)

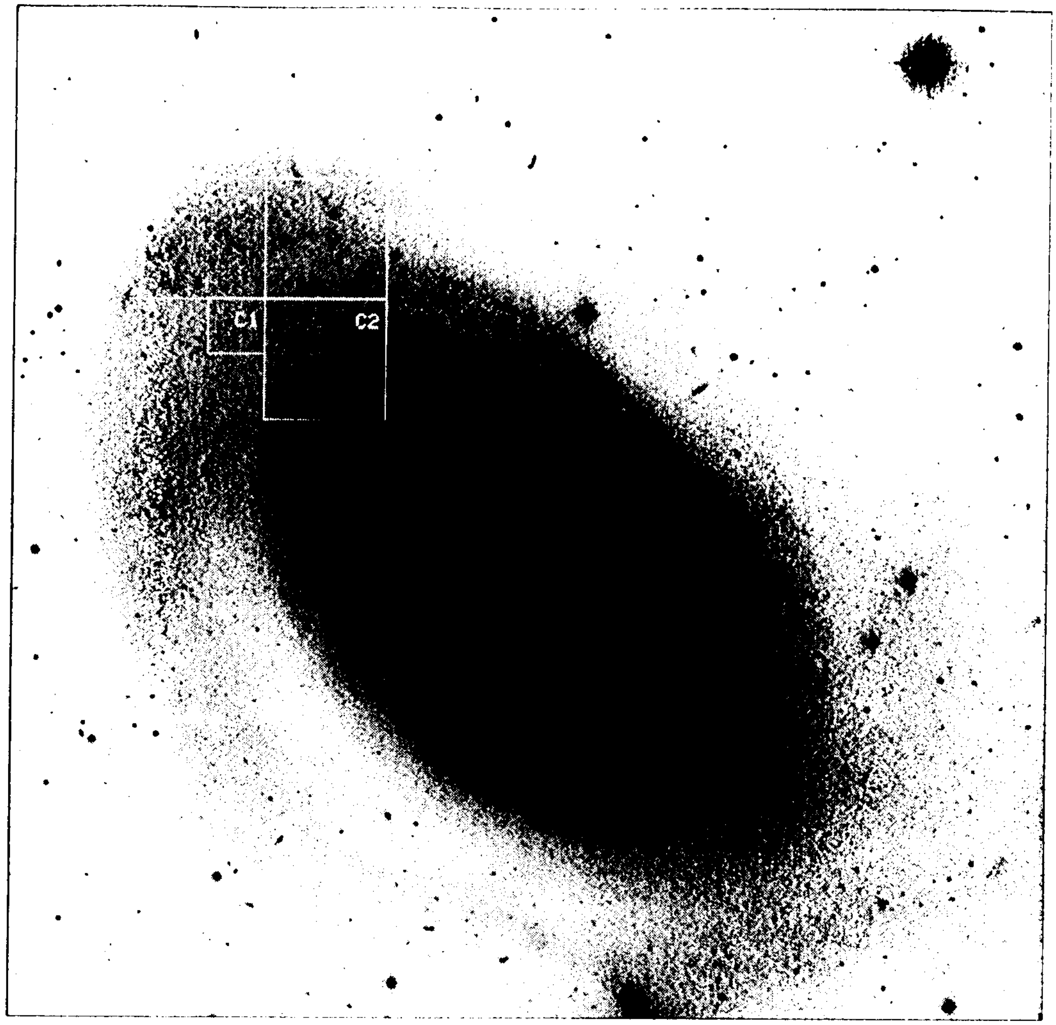
C1
C2

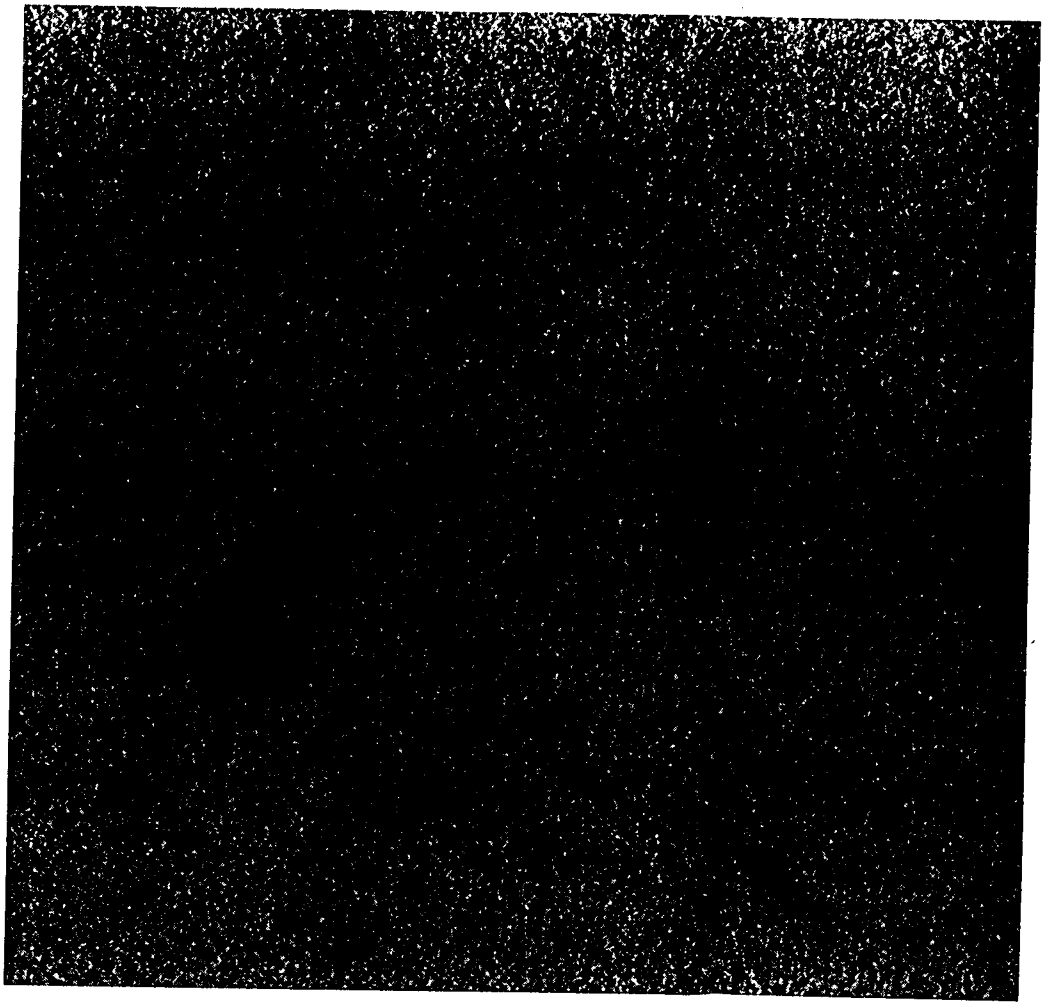

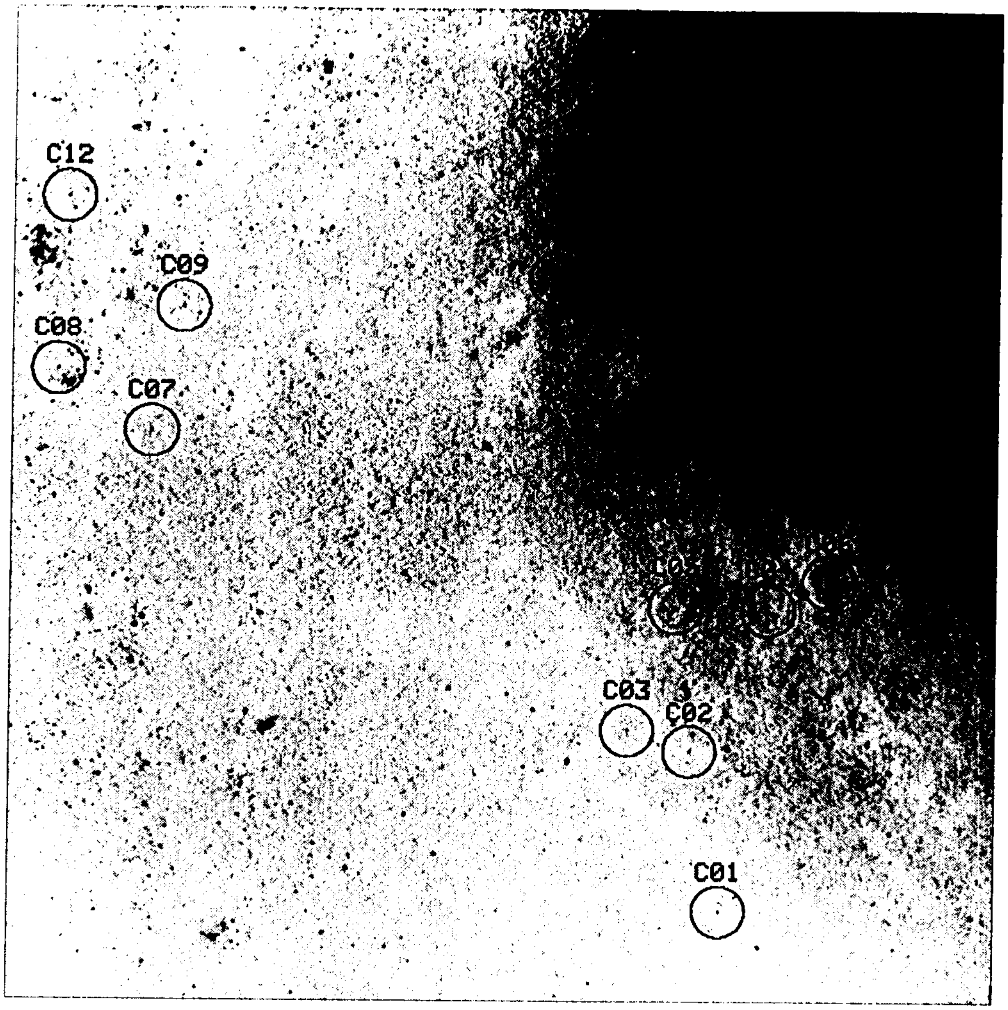
C12
C09
C08
C07
C03
C02
C01

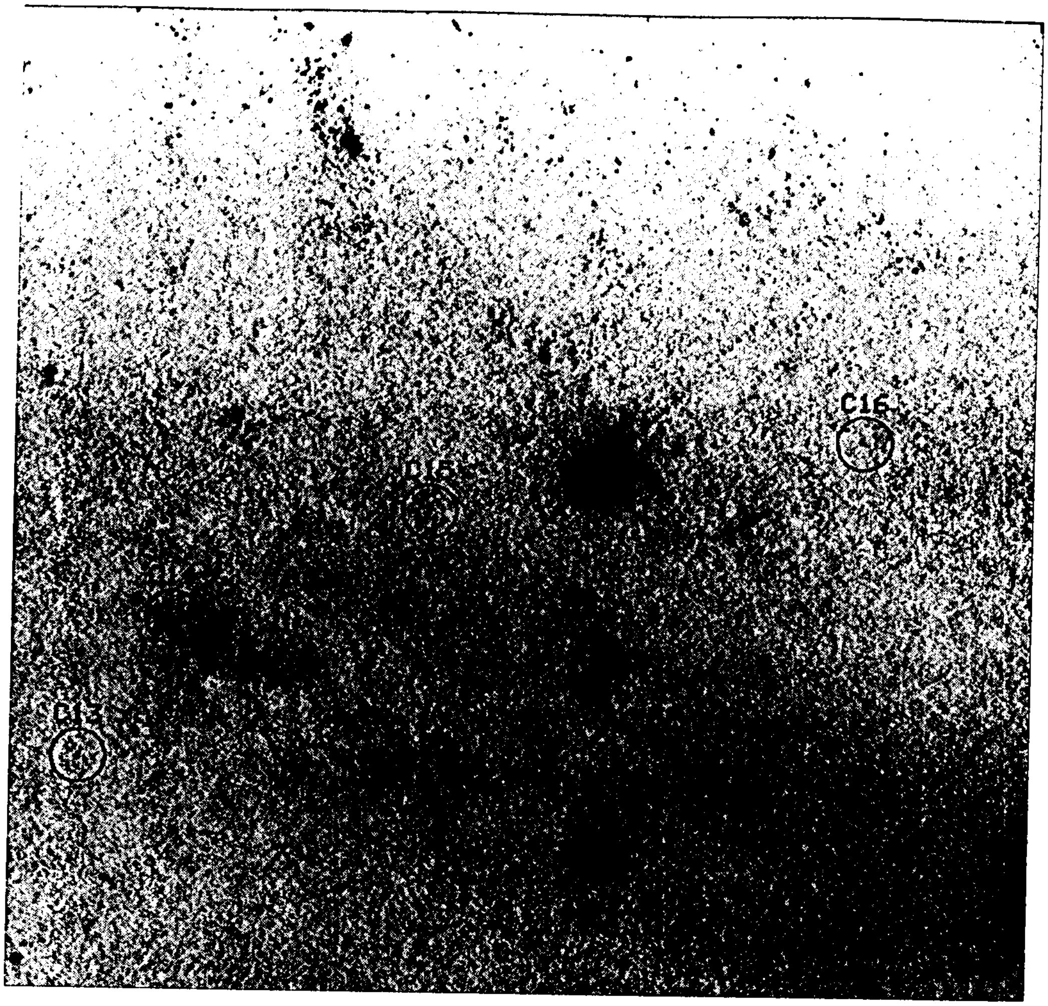
C16
C13

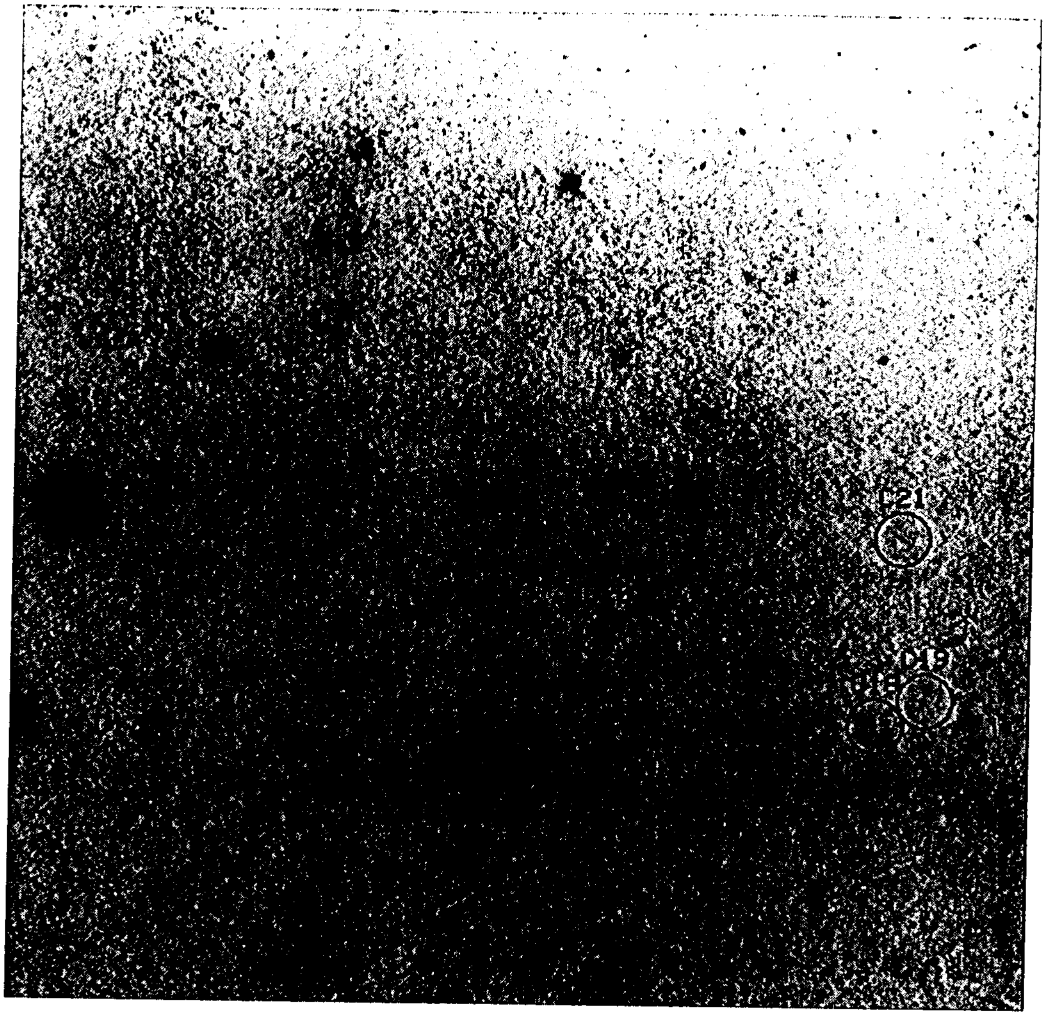
21
19
18

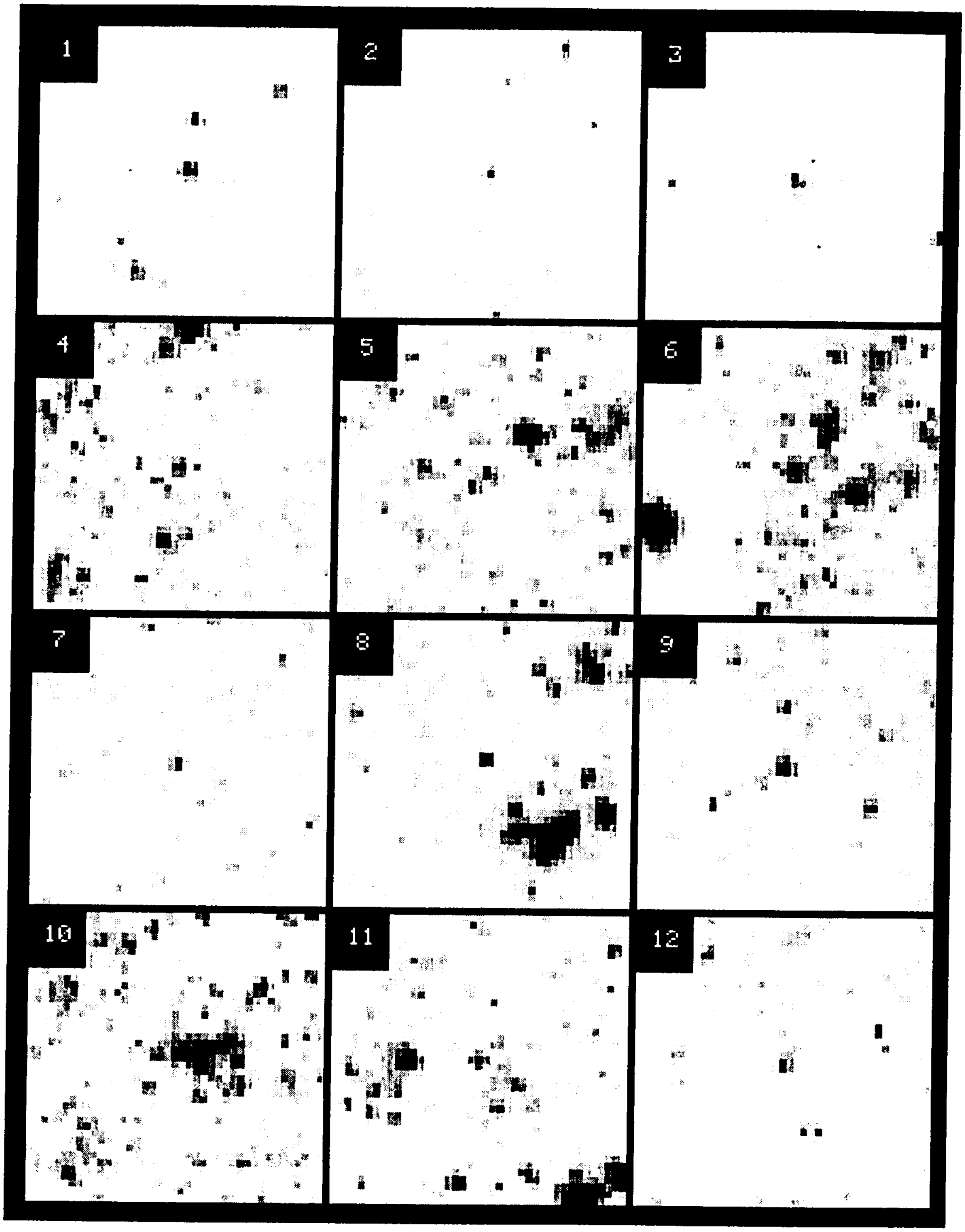
1
2
3
4
5
6
7
8
9
10
11
12

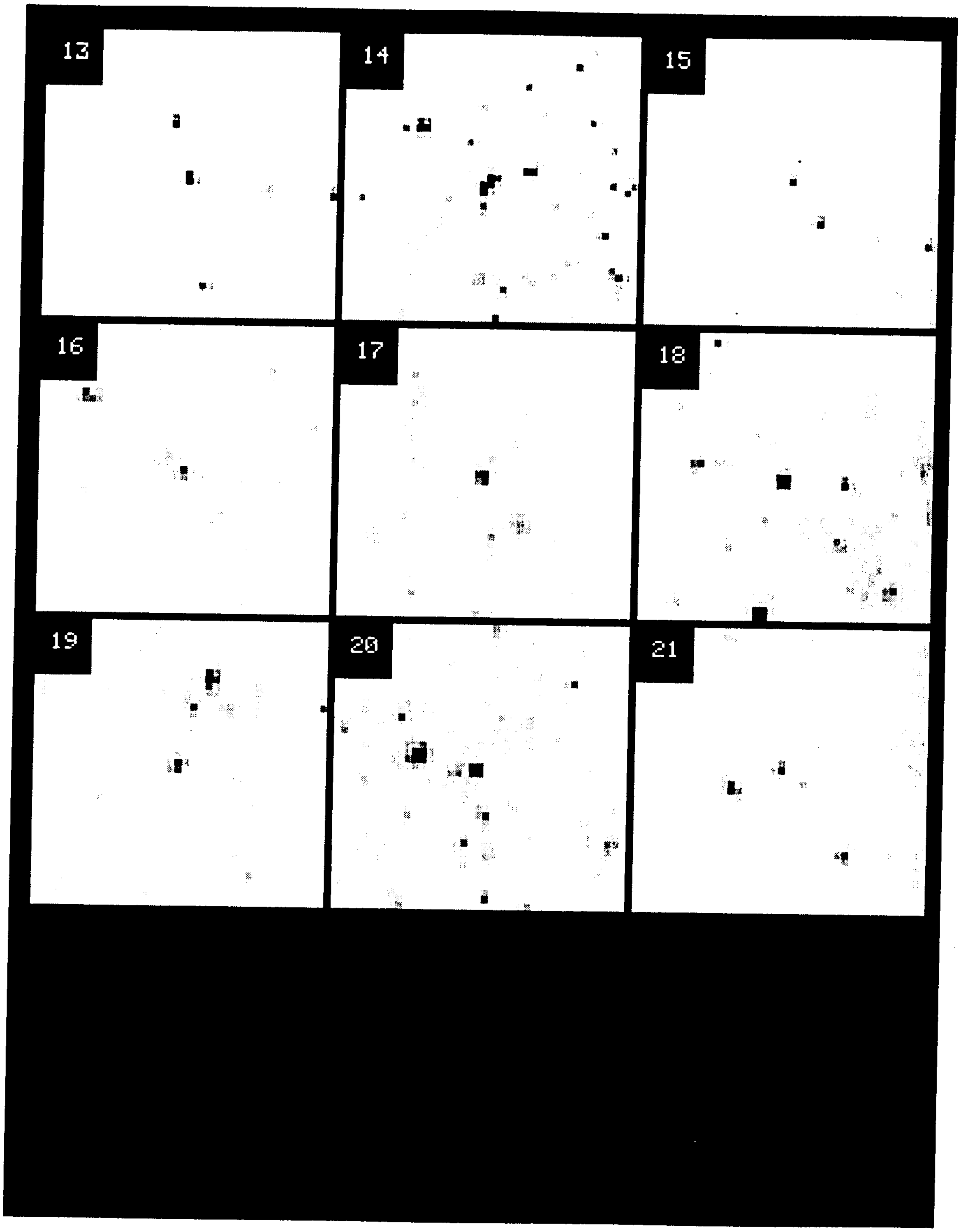
13
14
15
16
17
18
19
20
21

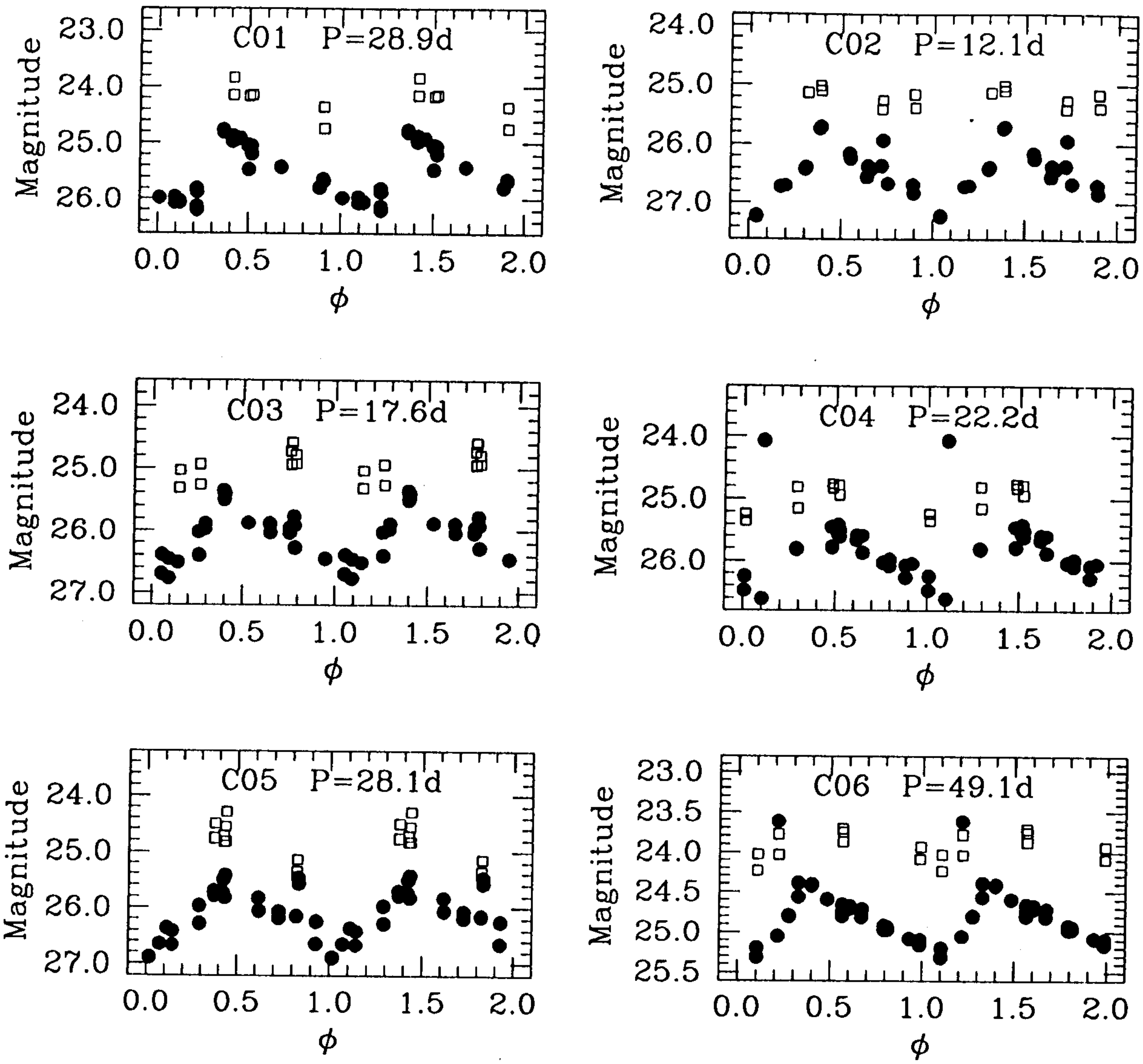
C01 P=28.9d
C02 P=12.1d
C03 P=17.6d
C04 P=22.2d
C05 P=28.1d
C06 P=49.1d
Magnitude
φ
0.0 0.5 1.0 1.5 2.0

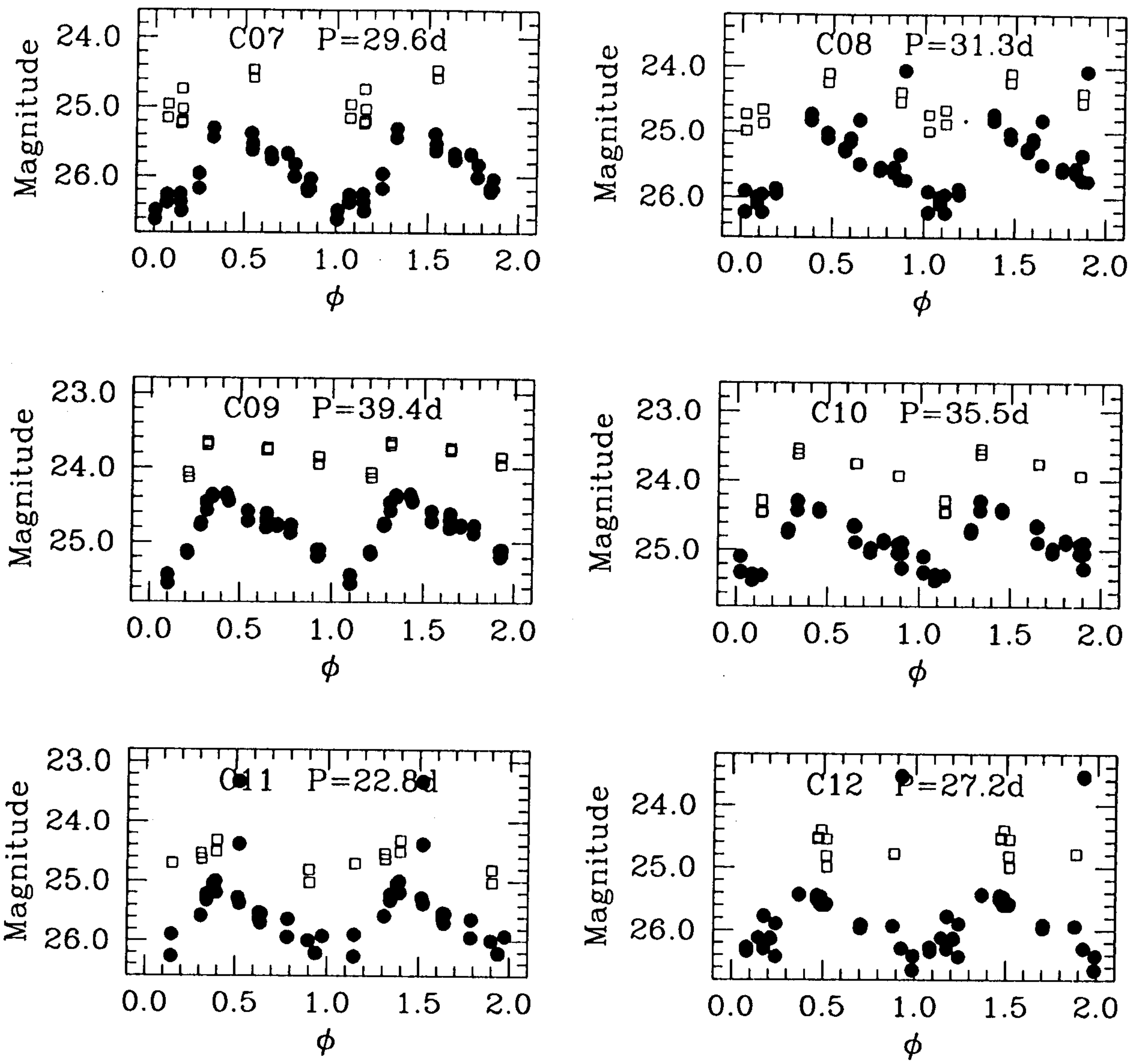
C07 P=29.6d
C08 P=31.3d
C09 P=39.4d
C10 P=35.5d
C11 P=22.8d
C12 P=27.2d
Magnitude
φ
0.0
0.5
1.0
1.5
2.0
23.0
24.0
25.0
26.0

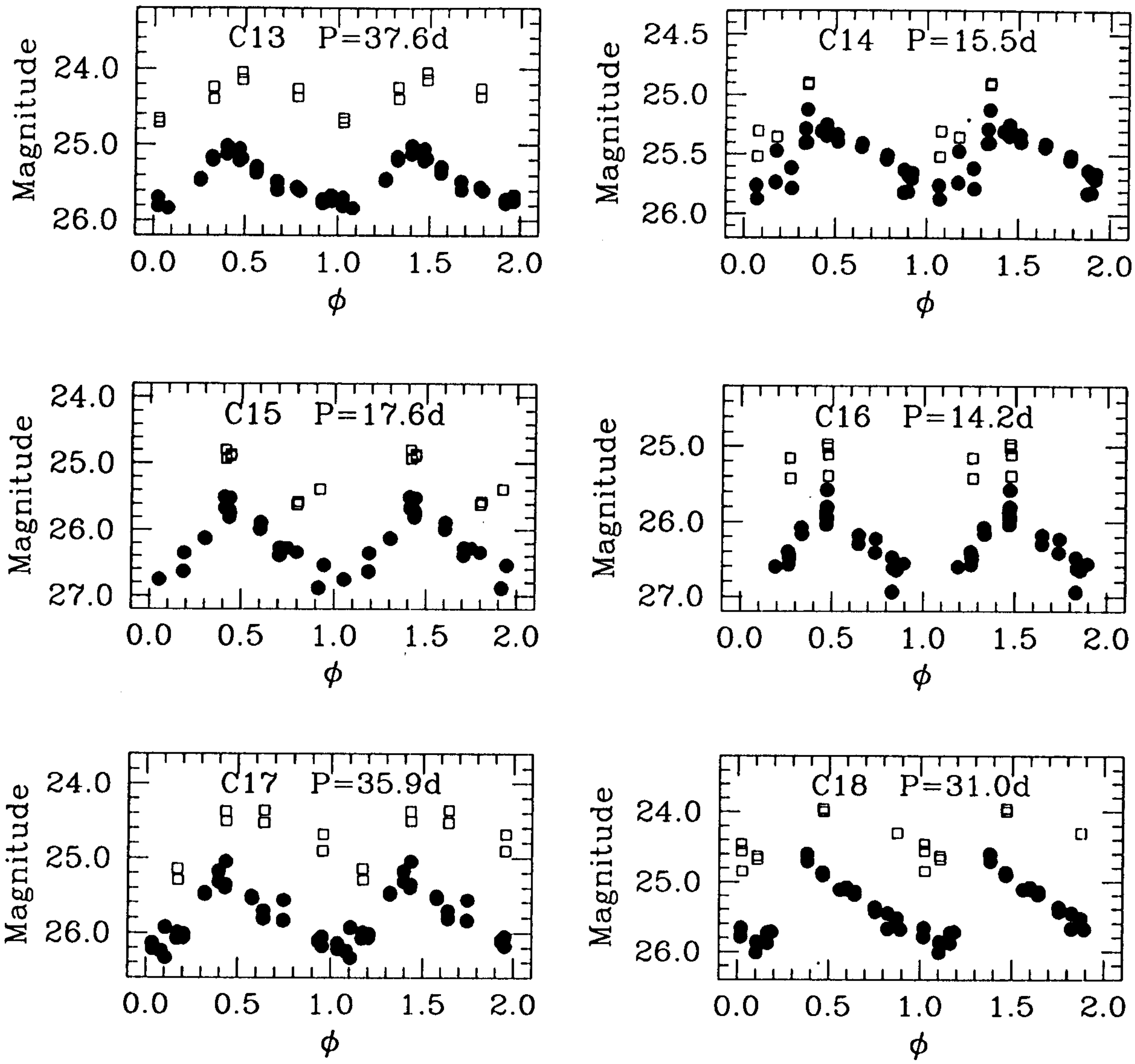
C13 P=37.6d
C14 P=15.5d
C15 P=17.6d
C16 P=14.2d
C17 P=35.9d
C18 P=31.0d
Magnitude
ϕ

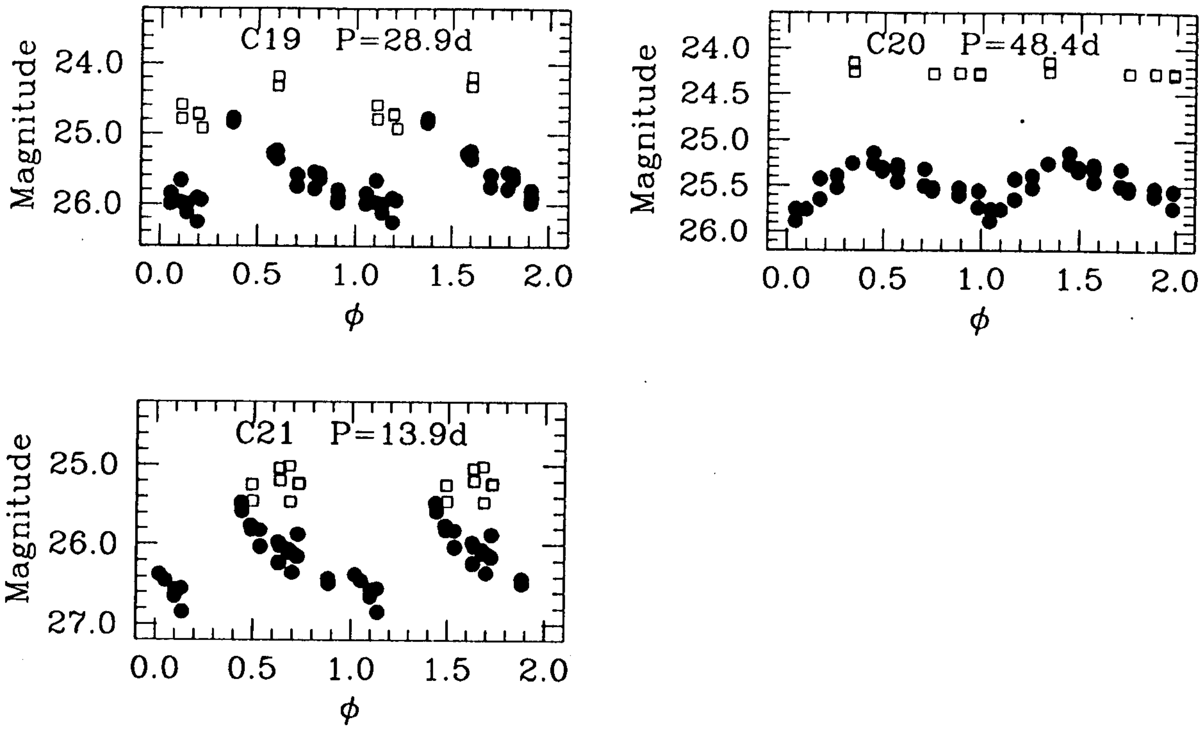
C19 P=28.9d
Magnitude
24.0
25.0
26.0
0.0 0.5 1.0 1.5 2.0
ϕ
C20 P=48.4d
Magnitude
24.0
24.5
25.0
25.5
26.0
0.0 0.5 1.0 1.5 2.0
ϕ
C21 P=13.9d
Magnitude
25.0
26.0
27.0
0.0 0.5 1.0 1.5 2.0
ϕ

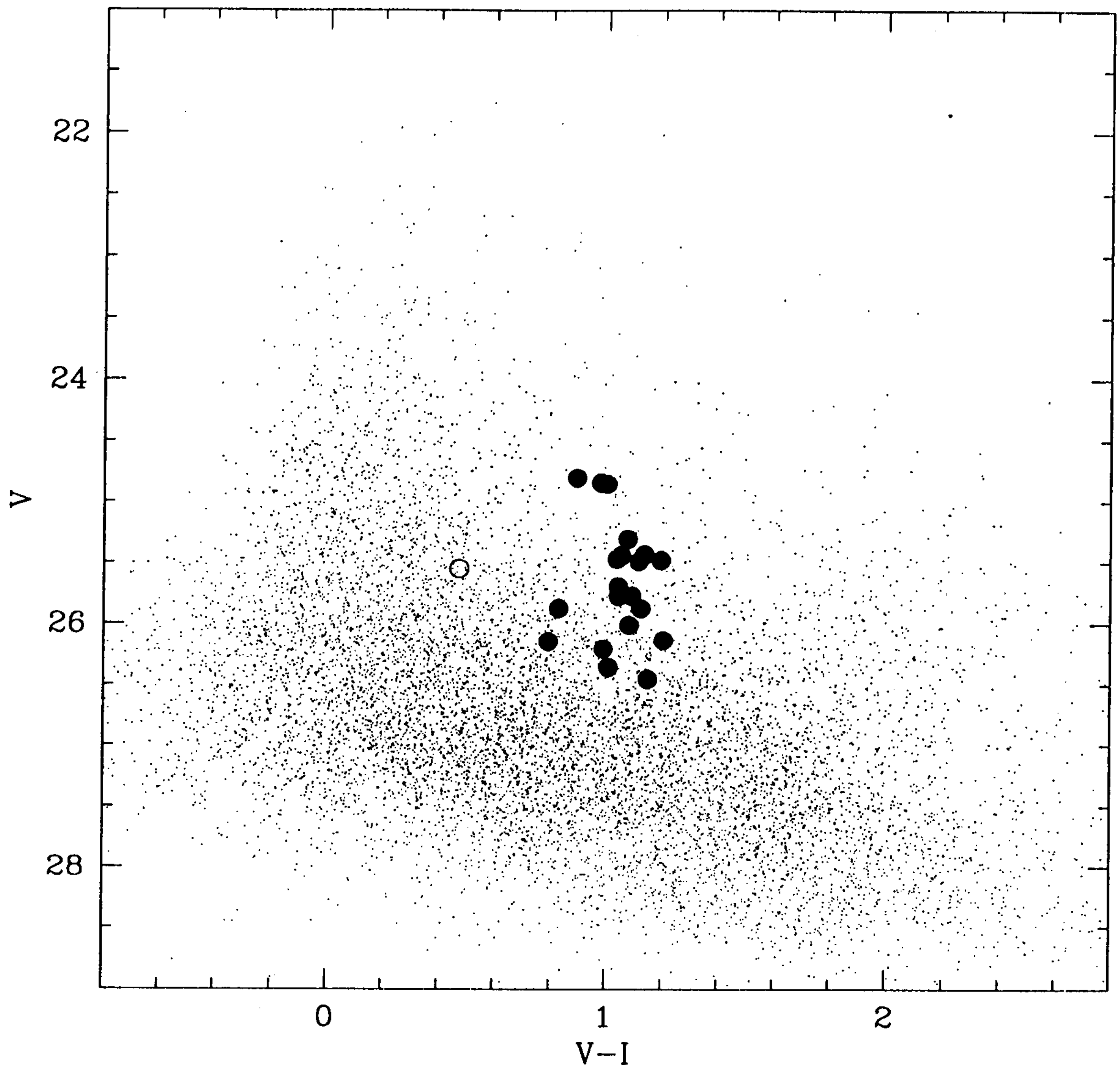
22
24
26
28
V
0
1
2
V–I

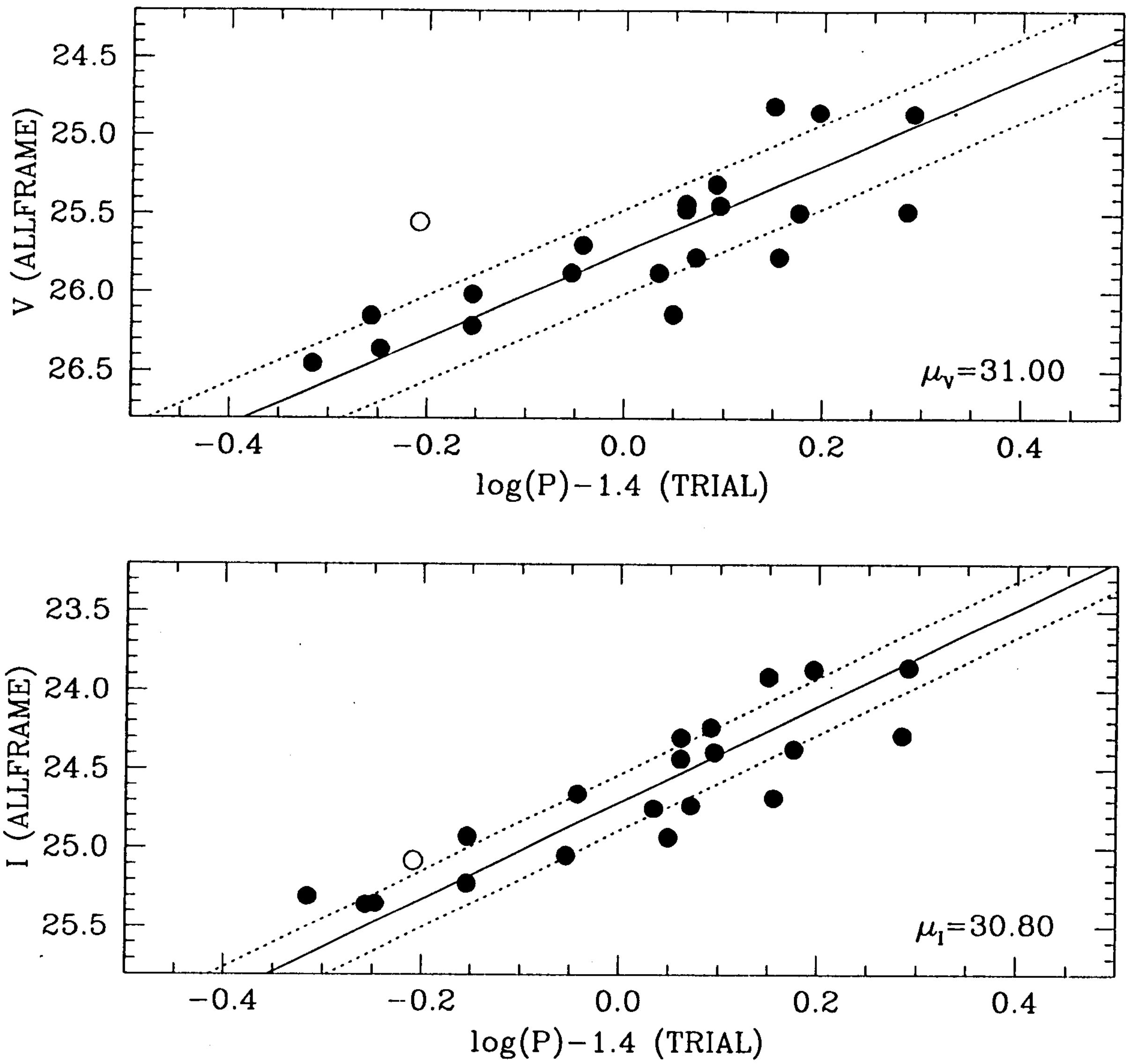
24.5
25.0
25.5
26.0
26.5
V (ALLFRAME)
μ_V=31.00
−0.4
−0.2
0.0
0.2
0.4
log(P)−1.4 (TRIAL)
23.5
24.0
24.5
25.0
25.5
I (ALLFRAME)
μ_I=30.80
−0.4
−0.2
0.0
0.2
0.4
log(P)−1.4 (TRIAL)

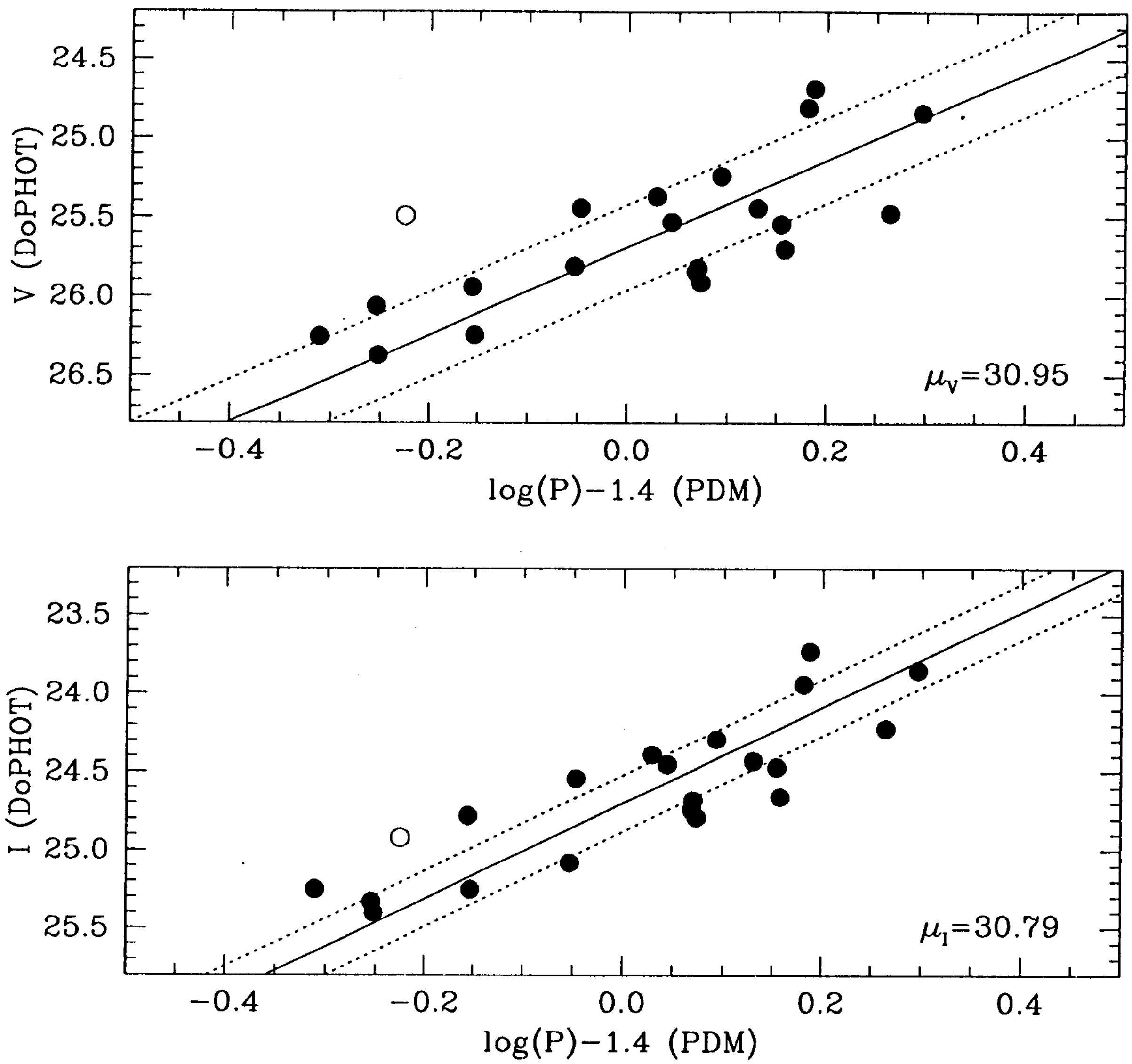
24.5
25.0
25.5
26.0
26.5
V (DoPHOT)
−0.4
−0.2
0.0
0.2
0.4
log(P)−1.4 (PDM)
μ_V=30.95
23.5
24.0
24.5
25.0
25.5
I (DoPHOT)
−0.4
−0.2
0.0
0.2
0.4
log(P)−1.4 (PDM)
μ_I=30.79

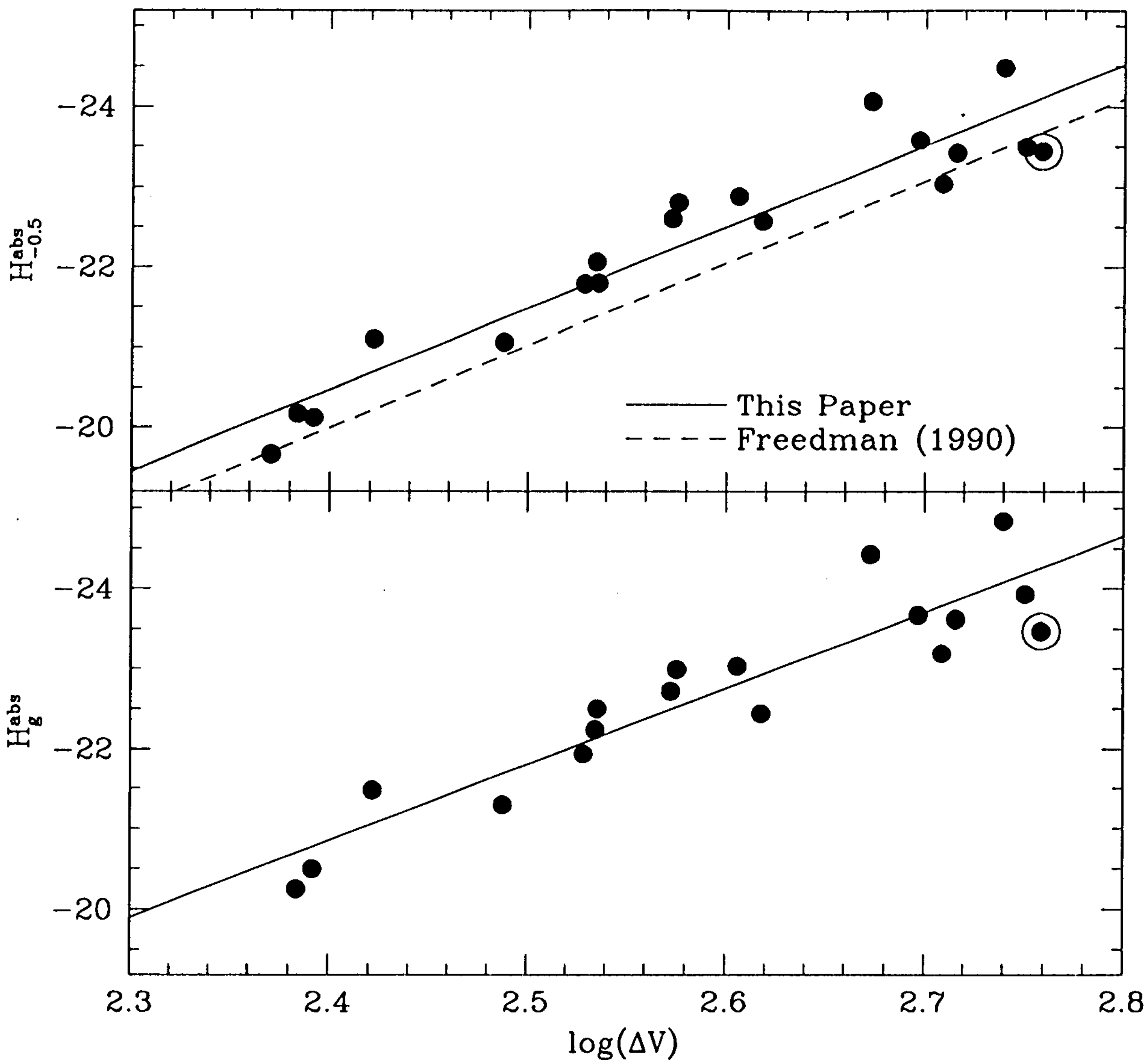

−24
−22
−20
$H^{abs}_{-0.5}$
This Paper
Freedman (1990)
−24
−22
−20
H^{abs}_{g}
2.3
2.4
2.5
2.6
2.7
2.8
log(ΔV)

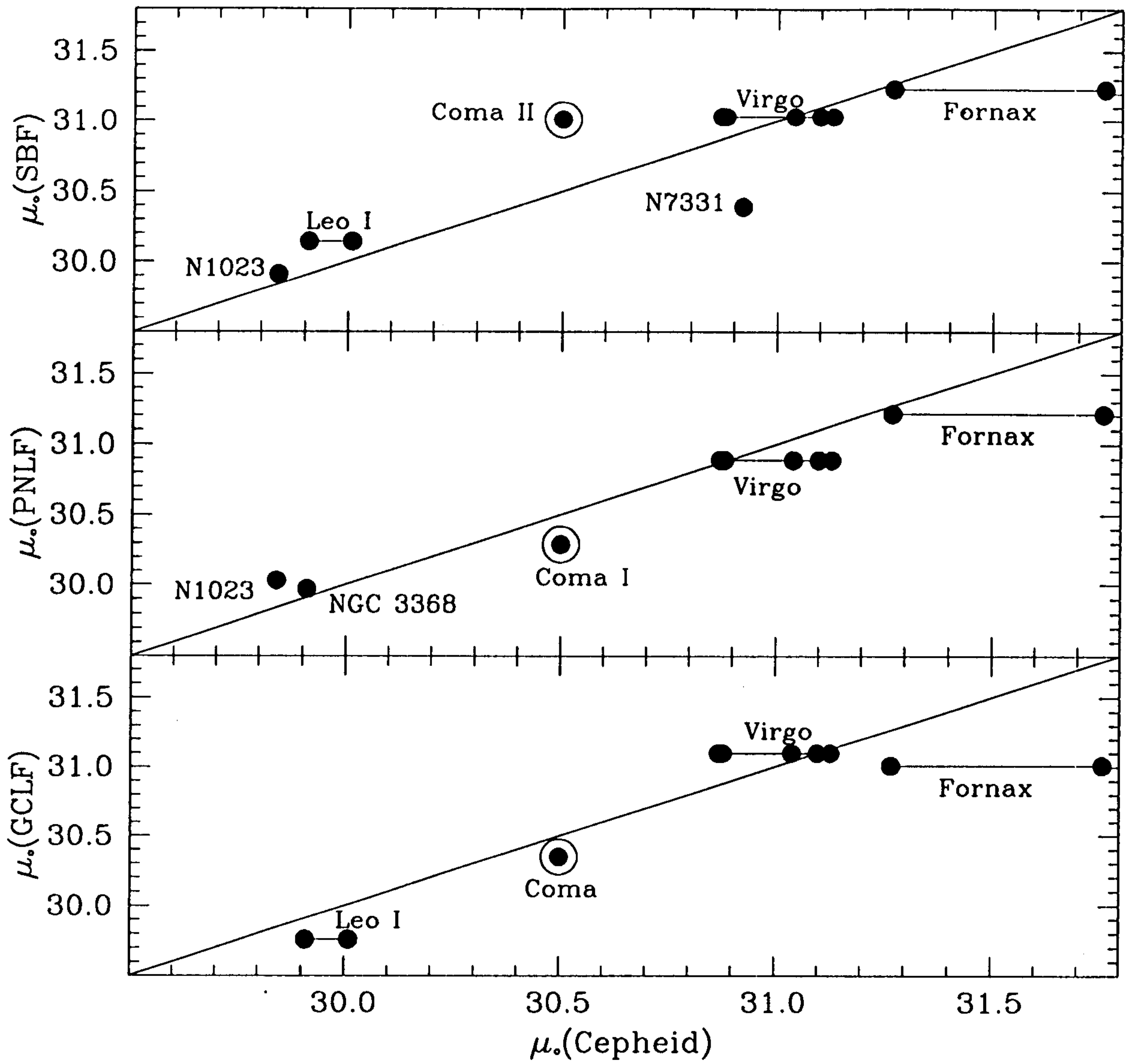
31.5
31.0
30.5
30.0
$\mu_\circ$(SBF)
Coma II
Virgo
Fornax
N7331
Leo I
N1023
$\mu_\circ$(PNLF)
Fornax
Virgo
Coma I
N1023
NGC 3368
$\mu_\circ$(GCLF)
Virgo
Fornax
Coma
Leo I
30.0
30.5
31.0
31.5
$\mu_\circ$(Cepheid)